Ultrasonics 94 (2019) 131–144

Contents lists available at ScienceDirect

Ultrasonics

journal homepage: www.elsevier.com/locate/ultras

Reflection and refraction of plane waves at the loosely bonded common interface of piezoelectric fibre-reinforced and fibre-reinforced composite media

Amrita Das[a,*], Abhishek Kumar Singh[a], Prajnya Parimita Patel[b], Kshitish Ch. Mistri[c], Amares Chattopadhyay[a]

[a] Department of Applied Mathematics, Indian Institute of Technology (Indian School of Mines), Dhanbad, Jharkhand 826004, India
[b] Department of Mathematics, National Institute of Technology, Rourkela, Odisha 769008, India
[c] Department of Mathematics, Chandrapur College, Burdwan, West Bengal 713145, India

ARTICLE INFO

Keywords:
Reflection and refraction
Piezoelectricity
Reinforced Composite
Loosely bonded
Initial stresses

ABSTRACT

The rapid development of the modern age has increased the urge of using composite structures having applications in the realm of various engineering fields. Specifically, fibre-reinforced piezoelectric composites are in the forefront of the present era because of its light weight, great strength and hence improved performance over the piezoelectric materials alone. Therefore, the present paper delves with the problem of reflection and refraction of plane waves when it is incident at the interface of a Piezoelectric Fibre-reinforced Composite (PFRC) medium and Fibre-reinforced Composite (FRC) medium. It is assumed that the media are loosely bonded to each other and are under horizontal initial stresses. It is established that the boundary conditions are satisfied by the set of three coupled waves associated with the PFRC medium (namely quasi-longitudinal wave (qP), quasi-transverse wave (qSV), electrostatic wave (EA)) and two coupled waves associated with the FRC medium (namely quasi-longitudinal wave (qP), quasi-transverse wave (qSV)). The amplitude ratio of reflected and refracted waves are obtained with the aid of suitable boundary conditions at the common interface of the two media. The effect of anisotropy, initial stresses and loose bonding on the amplitude ratio are studied numerically and demonstrated by means of graphs. The effect of anisotropy is also studied on the slowness curves, plotted in slowness surface. Moreover, the relation for energy partition is also derived and it is established that the total normal energy flux balance at the interface is unity.

1. Introduction

Propagation of elastic waves in a material medium may be accompanied with some sort of barrier causing the scattering phenomenon. If the barrier is the interface of two media with different properties then, the scattered waves include the reflected waves in the medium itself and refracted waves in the continuing media. The study of propagation behaviour of these waves may provide information about the source of generation of the waves, the material medium they pass through, the internal structure of the earth and exploration of valuable minerals buried. Moreover, anisotropy in material medium is among the common features of most constructions which may lead to significant distortions in conventional elastic processing, including the occurrence of errors in velocity analysis, disturbed reflections and amplitude variation with offset response. Therefore, the presence of anisotropy in the medium suggest that the incident, reflected and transmitted waves are no longer purely longitudinal or shear in nature rather they may be categorised as qP-, qSH-, qSV- waves (instead of P-, SH- and SV- waves respectively), all three propagating with three different velocities and mutually orthogonal particle motion [1]. In the past few years, the problems of reflection and refraction of elastic waves have gained much of researcher's attention in view of both theoretical investigations and applications in the field of acoustics, non-destructive evaluation and mining in oil industries. It is well established that anisotropy and initial stresses have substantial effect on the propagation of three-dimensional plane wave when it is incident at the common interface of anisotropic media [2–6].

In general, the contact between two media is assumed to be welded (perfectly bonded) for solving the problems of elastic wave propagation through them. The assumption imposes the continuity of stresses and

* Corresponding author.
E-mail address: amritadas.ism@gmail.com (A. Das).

https://doi.org/10.1016/j.ultras.2018.11.008
Received 12 April 2018; Received in revised form 24 September 2018; Accepted 25 November 2018
Available online 27 November 2018
0041-624X/

displacements across the common interface. On the other hand, the two continuing media may be in ideally smooth contact which results in an infinite slip implying the condition of vanishing of shearing stress at the interface. In between these two cases, there are possibilities that the two media are loosely (imperfectly) bonded to each other. A loosely bonded interface allows a finite amount of slip for the material motion which implies the existence of a relation between the local shearing stress and the 'slip'. The contemplation of loosely bonded interface find numerous applications in construction engineering. Murty [7,8] established the secular equation of Stoneley wave when it propagates through two loosely bonded isotropic elastic half-spaces. The effect of loosely bonded interfaces on the propagation, reflection and transmission of elastic waves is investigated by many researchers [9–13].

Nowadays, the lightweight fibre-reinforced materials find a number of engineering applications because of its great strength and stiffness. Consequently, efforts are made in recent years towards the development of such materials, technologically, for their effective utilization in numerous fields including construction (buildings, towers, and bridges), aviation, space, sports and medical service, and leisure fields. The mechanical property of these materials aids to minimize the damage resulting from an effect of vibration. Accurate designing of heavy civil construction projects requires the intense study of propagation behaviour of waves so as to understand and predict the nature and sources of ground movement. Fibre-reinforced materials are composed of the fibres and the matrix which are bound together in such a way that there is no relative displacement between them. As a result the constituent components of the material act as a single unit under elastic condition. Carbon, nylon, or conceivable metal whiskers are good examples of these type. Singh [14] obtained the frequency equation for the propagation of plane waves in a fibre-reinforced thermoelastic media. The propagation behaviour of magnetoelastic shear waves in self-reinforced layer with irregularity is discussed by Chattopadhyay and Singh [15]. Samal and Chattaraj [16] demonstrated the effect of reinforcement on surface wave propagation in a sandwiched anisotropic elastic layer. Singh et al. [17] established that reinforced layer supports more to the phase velocity of Love-type wave as compare to reinforced free layer when it propagates through a corrugated fibre-reinforced layer.

Simultaneously, the numerous applications of piezoelectric materials viz. accelerometers, microphones, ultrasonic transducers and advanced engineering applications like aerospace, space explorations, automatic remote control, came into light in the past decades. These materials are widely used for controlling the vibration of light weight smart structures in distributed sensors and/or actuators. Meanwhile, it became a great deal in research to model the engrossing electromechanical behaviour of piezoelectric materials. In spite of their great applications, the piezoelectric materials including PZT, PVDF and barium titanate, have certain limitations, like low piezoelectric constants, shape control (due to their weight) and high specific acoustic impedance, which are responsible for lowering the control authority of the distributed actuators. Hence, keeping in view the strength and lightweight property of fibre-reinforced materials, these limitations are vanquished with the use of fibre-reinforced piezoelectric composites. Mediums constituted with $BaTiO_3$ and $CoFe_2O_4$ also exhibit piezoelectric behaviour. Pang et al. [18] analyses the reflection and refraction of a plane wave when it is incident at the interface between piezoelectric and piezomagnetic media composed of $BaTiO_3$ and $CoFe_2O_4$, respectively. Later, Pang and Liu [19] extended the study by taking imperfectly bonded interface. Materials exhibiting piezoelectric behaviour also include PZT-5H ceramics, barium titanate ceramics, silicon dioxide glass, borosilicate glass, cobalt iron oxide and aluminium nitride. Singh et al. [20] adopted the Green's function technique to obtain the expression for particle displacements due to SH-wave propagating in a transversely isotropic piezoelectric layer under the influence of a point source.

Piezoelectricity is nothing but a reversible process where energy is transferred from the mechanical domain to the electrical domain and vice versa. The low magnitude of piezoelectric stress/strain coefficients causes the poor performance of smart structures. Particularly, for the case when a unit electric field is applied across the thickness of the piezoelectric actuator, the induced normal stress in the longitudinal direction is measured by the piezoelectric constant e_{31}. Hence, the magnitude of e_{31} must be modified to improve the control authority of the distributed piezoelectric actuators. Thus, the fibre-reinforced piezoelectric composites are designed so that an improved value of the effective piezoelectric constant may be achieved.

Fibre-reinforced piezoelectric composites have improved performance over the piezoelectric materials alone and, currently, are widely being used in underwater transducers and medical imaging applications. Ray [21] described the micromechanics of piezoelectric composites with improved effective piezoelectric constants. Mallik and Ray [22] obtained the coefficients of piezoelectric fiber-reinforced composites. The effective properties of thermo-electro-mechanically coupled piezoelectric fiber reinforced composites were marked by Kumar and Chakraborty [23]. Numerical methods are also developed for solving problems concerning these materials [24–27].

The piezoelectric materials are usually made initially stressed or pre-stressed so as to prevent it from brittle fracture. Apart from this, the different material properties (viz. thermal expansion, shrinkage and growth) at different temperature reasserts the necessity of consideration of initial stress in the problems concerning piezoelectric materials. Therefore, the study of pre-stressed structures is of importance, and the reflection and refraction of plane waves is a convenient tool for this task. Some notable works considering the effect of initial stress on the propagation of elastic wave include Singh et al. [28], Singh and Yadav [29], Guz [30], Khurana and Vashisth [31].

Till date, no attempt has been made to study the reflection and refraction of plane waves in piezoelectric fibre-reinforced composite overlaying a fibre-reinforced medium. Therefore, the present paper undertook to study the effect of anisotropy, loose bonding and initial stresses on the reflection and refraction of plane waves at the interface of a Piezoelectric Fibre-reinforced Composite (PFRC) medium and Fibre-reinforced Composite (FRC) medium. With the aid of suitable boundary conditions at the common interface, the amplitude ratio corresponding to the reflected qP wave, reflected qSV wave, reflected EA wave, refracted qP wave and refracted qSV wave are derived. Numerical computation is performed to study the effect of initial stresses and loose bonding on the amplitude ratio by taking the suitable data of PZT-5H material. Moreover, the effect of anisotropy on the amplitude ratio is exhibited by means of comparative study through graphical illustrations in various cases.

2. Basic assumptions

2.1. Basic assumptions for the loosely bonded common interface

Keeping in view the objective of the proposed study, it is needful to analyze the numerical value to be assigned to the bonding parameter corresponding to the degree of bonding between two media. The three basic assumptions for the purpose are as follows [7,8]:

- The stresses across the common interface of the two media are continuous.
- A finite amount of slip can take place in microscopic level at the interface of the two media when a periodic wave is propagating through it.
- The finite slip at the interface of the two media is proportional to the local shearing stress i.e. shearing stress at the interface= $T\times$slip; where T is the proportionality constant.

The first two assumptions are involved in the study of dislocations in solids and wave motion at the smooth interface between two media;

while the third assumption indicates relationship between the local shearing stress and the 'slip'. For the case when the interface of two media is ideally smooth, 'slip' is infinite; and the 'slip' vanishes for the case when the two media are perfectly bonded. Mathematically,

- $T = 0$, implies that the interface of the media is ideally smooth.
- $T \to \infty$, implies that the interface is welded.
- $0 < T < \infty$, implies that the interface is loosely bonded.

The loose bonding of the two media may arise due to the presence of an infinitesimal thin viscous layer at the common interface. The thickness of this viscous layer 'h' is assumed to be infinitely small i.e. $h \to 0$. Assuming χas the coefficient of viscosity of the viscous layer, the shearing stress (σ_{13}^{c}) at the interface may be written as

$$\sigma_{13}^{c} = \chi u_{1,x_3 t}, \tag{1}$$

$u_{1,t}$ being the time (t) derivative of the displacement component parallel to the interface and superscript 'c' stands for composite material associated with the PFRC medium.

Assuming the waves to be time harmonic in nature and the jump of velocity across the viscous layer as $(u_{1,t} - v_{1,t})$, Eq. (1) may be rewritten as

$$\sigma_{13}^{c} = i\omega\frac{\chi}{h}(u_1 - v_1), \tag{2}$$

where ω is the angular frequency, and u_1 and v_1 are the components of displacement of the PFRC and FRC mediums, respectively, parallel to the interface at the boundaries of the infinitesimal thin viscous layer.

2.2. Micromechanics model for the PFRC medium

The PFRC medium is assumed to be comprised of a number of piezoelectrically active fibres which are surrounded by the piezoelectrically inactive matrix material. The composite is taken in such a way that there is no slippage between fibres and the matrix. It is assumed that the fibres of the considered homogeneous composite are continuous and oriented longitudinally in x_1−direction. The polling direction of the fibres is parallel to axis. Also, the fibre as well as the matrix are assumed to be linearly elastic. Both fibre and matrix are included in the representative volume of the micromechanical model [21]. Therefore, the PFRC is an assembly of rectangular representative volume elements which contains both fibre and matrix inducing that the effective properties of the PFRC would be same as that of the representative volume elements [23].

In addition to these assumptions for the micromechanical model, it is assumed that the electric field is applied across the thickness of the composite so as to maintain a constant electric field in fibres, keeping the piezoelectric fibres along the horizontal direction. It is of ease to maintain a constant electric field across the composite of less thickness. Moreover, the electric field and temperature change is maintained equally in both fibres and the matrix.

3. Geometrical model of the problem

The problem of reflection and refraction of plane waves at the interface of a PFRC medium (say mediumM_1) and a FRC medium (say mediumM_2), both under initial stress is considered in the present study. It is assumed that the two media are loosely bonded to each other. The problem delves with incident and reflected qP, qSV and EA waves in the PFRC medium and refracted qP and qSV waves in the FRC medium.

The electroacoustic (EA) wave is the acoustic wave propagating in piezoelectric solid accompanied by quasi-static electric fields due to the electromechanical coupling effect. In order to solve the problem, Cartesian co-ordinate system is assumed in such a way that x_1−axis is along the common interface of the half-spaces, axis is positively pointing downwards and origin 'O' is at the point of incidence of the plane wave on the common interface at x_1−axis (Fig. 1).′

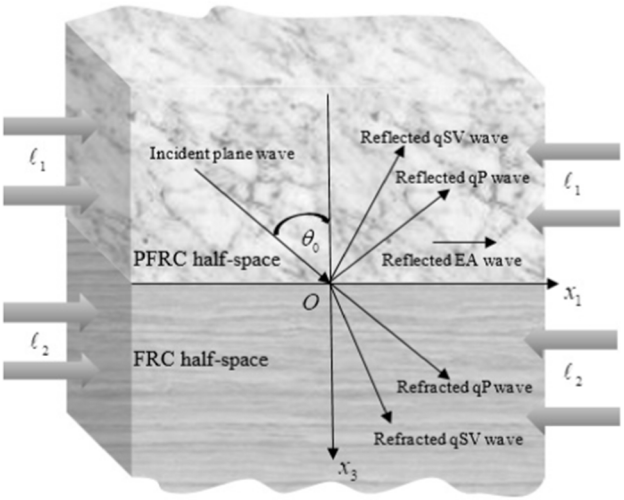

Fig. 1. Geometrical model of the problem.

4. Propagation conditions and constitutive relations

While dealing with the case of plane strain in a co-ordinate system as shown in Fig. 1, the displacement components and electric potential may only be written as the function of x_1 and x_3. Therefore, for the propagation of plane waves in PFRC medium, it may be written that

$$u_1 = u_1(x_1, x_3, t),\ \ u_2 = 0,\ \ u_3 = u_3(x_1, x_3, t) \text{and} \phi = \phi(x_1, x_3, t), \tag{3}$$

where u_1, u_2 and u_3 are the components of displacement in PFRC medium in x_1, x_2 and x_3 directions respectively; and ϕ is the scalar potential.

For the propagation of plane waves in FRC medium, the displacement components may be written as

$$v_1 = v_1(x_1, x_3, t),\ \ v_2 = 0,\ \ v_3 = v_3(x_1, x_3, t), \tag{4}$$

where v_1, v_2 and v_3 are the components of displacement in FRC medium in x_1, x_2 and x_3 directions respectively.

4.1. Constitutive relations for the PFRC medium

Assuming that the electric field is acting only in direction, the constitutive equations for the piezoelectrically active fibres of the composite material may be given as [22]

$$\begin{bmatrix} \sigma^f \\ \mathbf{D}^f \end{bmatrix} = \begin{bmatrix} \mathbf{C}^f & \mathbf{e}^f \\ (\mathbf{e}^f)^{\mathrm{T}} & \xi^f \end{bmatrix} \begin{bmatrix} \varepsilon^f \\ \mathbf{E}^f \end{bmatrix}, \tag{5}$$

where $(\boldsymbol{e}^f)^{\mathrm{T}}$ is the transpose of $\boldsymbol{e}^f$. On the other hand, the constitutive equations for the piezoelectrically inactive matrix of the composite material may be written as

$$\begin{bmatrix} \sigma^m \\ \mathbf{D}^m \end{bmatrix} = \begin{bmatrix} \mathbf{C}^m & 0 \\ 0 & \xi^m \end{bmatrix} \begin{bmatrix} \varepsilon^m \\ \mathbf{E}^m \end{bmatrix}. \tag{6}$$

In the above set of Eqs. (5) and (6), the superscript 'f' stands for fibre and 'm' stands for the matrix phase of the composite material.

Now, in reference to the basic assumptions for the micromechanics model of fibre-reinforced composite medium, Eqs. (5) and (6) jointly give the resultant constitutive equation for the PFRC medium as

$$\begin{bmatrix} \sigma^c \\ \mathbf{D}^c \end{bmatrix} = \begin{bmatrix} \mathbf{C}^c & \mathbf{e}^c \\ (\mathbf{e}^c)^{\mathrm{T}} & \xi^c \end{bmatrix} \begin{bmatrix} \varepsilon^c \\ \mathbf{E}^c \end{bmatrix}, \tag{7}$$

where $\boldsymbol{e}^c = \boldsymbol{e}^f$. In general, $\boldsymbol{\sigma}$ and $\boldsymbol{\varepsilon}$ are the stress and strain vectors, respectively; $\boldsymbol{D}$ and $\boldsymbol{E}$ are the electric displacement and electric field,

respectively; $\boldsymbol{C}$, $\boldsymbol{e}$ and $\boldsymbol{\xi}$ are the elastic, piezoelectric and dielectric constants, respectively. The mathematical representation of these vector matrices are provided in Appendix.

The assumption that there is no slippage at the fibre-matrix interface, implies that the fibre and the matrix are perfectly bonded constituting the composite material. Therefore, the average normal strains in x_1−direction are same in fibre, matrix and the PFRC material, i.e.$\varepsilon_{11}^f = \varepsilon_{11}^m = \varepsilon_{11}^c$. Also, the average normal strains in x_2− and directions and the average shear strains may be expressed by employing the rule of mixtures as follows [32]:

$$\left.\begin{aligned} \varepsilon_{22}^c = \Lambda_f\varepsilon_{22}^f + \Lambda_m\varepsilon_{22}^m, \quad \varepsilon_{33}^c = \Lambda_f\varepsilon_{33}^f + \Lambda_m\varepsilon_{33}^m, \quad \varepsilon_{23}^c = \Lambda_f\varepsilon_{23}^f + \Lambda_m\varepsilon_{23}^m,\\ \varepsilon_{13}^c = \Lambda_f\varepsilon_{13}^f + \Lambda_m\varepsilon_{13}^m, \quad \varepsilon_{12}^c = \Lambda_f\varepsilon_{12}^f + \Lambda_m\varepsilon_{12}^m, \end{aligned}\right\} \tag{8}$$

where Λ_f and Λ_m represents the volume fraction of fibre and matrix respectively.

For the sake of attaining equilibrium of axial forces, it requires that the average stress in x_1−direction in the composite material is expressed with the aid of rule of mixtures in terms of the average stresses in the fibre and matrix. Again for attaining equilibrium, the average stresses in x_2− and directions and all the shear stresses are considered same in the fibre and matrix and equal to the respective average stresses in the PFRC medium. Accordingly, the components of stress may be given as [33]

$$\left.\begin{aligned} \sigma_{11}^c = \Lambda_f\sigma_{11}^f + \Lambda_m\sigma_{11}^m, \quad \sigma_{22}^c = \sigma_{22}^f = \sigma_{22}^m, \quad \sigma_{33}^c = \sigma_{33}^f = \sigma_{33}^m,\\ \sigma_{13}^c = \sigma_{13}^f = \sigma_{13}^m, \quad \sigma_{23}^c = \sigma_{23}^f = \sigma_{23}^m, \quad \sigma_{12}^c = \sigma_{12}^f = \sigma_{12}^m. \end{aligned}\right\} \tag{9}$$

Now, keeping in view that the electric field in the fibre and the matrix are same, the resultant electric displacements in the PFRC medium in x_1, x_2 and directions may be expressed as

$$D_1^c = \Lambda_f D_1^f + \Lambda_m D_1^m,\ D_2^c = \Lambda_f D_2^f + \Lambda_m D_2^m,\ D_3^c = \Lambda_f D_3^f + \Lambda_m D_3^m. \tag{10}$$

4.2. Constitutive relations for the FRC medium

The constitutive equations for FRC medium with respect to a preferred direction $\vec{a}$ are [34]

$$\begin{aligned} \tau_{ij} = \lambda\zeta_{kk}\delta_{ij} + 2\mu_T\zeta_{ij} + \gamma(a_k a_m\zeta_{km}\delta_{ij} + a_i a_j\zeta_{kk})\\ + 2(\mu_L - \mu_T)(a_i a_k\zeta_{kj} + a_j a_k\zeta_{ki}) + \beta a_i a_j\zeta_{km}a_k a_m,\ i, j, k, m = 1, 2, 3 \end{aligned} \tag{11}$$

Newly introduced symbols in Eq. (11) are provided in Table 1.

Moreover, vector , denotes the preferred direction of reinforcement such that$\sum_{i=1}^{3} a_i^2 = 1$. The fiber direction is assumed parallel to x_1−axis. Therefore, $\vec{a}$ is so chosen that its components are (1, 0, 0).

5. Dynamics of the PFRC medium under initial stress

The expression for the components of stress and electric displacement in the PFRC medium may be written with the aid of Eq. (7) as

$$\left.\begin{aligned} \sigma_{11}^c = C_{11}^c\varepsilon_{11}^c + C_{12}^c\varepsilon_{22}^c + C_{13}^c\varepsilon_{33}^c - e_{31}^c E_3^c,\\ \sigma_{22}^c = C_{12}^c\varepsilon_{11}^c + C_{22}^c\varepsilon_{22}^c + C_{23}^c\varepsilon_{33}^c - e_{32}^c E_3^c,\\ \sigma_{33}^c = C_{13}^c\varepsilon_{11}^c + C_{23}^c\varepsilon_{22}^c + C_{33}^c\varepsilon_{33}^c - e_{33}^c E_3^c, \quad \sigma_{23}^c = 2C_{44}^c\varepsilon_{23}^c - e_{24}^c E_2^c,\\ \sigma_{31}^c = 2C_{55}^c\varepsilon_{31}^c - e_{15}^c E_1^c,\\ \sigma_{12}^c = 2C_{66}^c\varepsilon_{12}^c, \quad D_1^c = 2e_{15}^c\varepsilon_{31}^c + \xi_{11}^c E_1^c, \quad D_2^c = 2e_{24}^c\varepsilon_{23}^c + \xi_{22}^c E_2^c,\\ D_3^c = 2e_{31}^c\varepsilon_{11}^c + e_{32}^c\varepsilon_{22}^c + e_{33}^c\varepsilon_{33}^c + \xi_{33}^c E_3^c. \end{aligned}\right\} \tag{12}$$

Due to piezoelectricity and initial stress prevailing in the PFRC medium, the equations of motion, in absence of body forces may be written as

$$\sigma_{ij,j}^c + (u_{j,k}\ell_{ki})_{,i} = \rho_1^c u_{i,tt}, \quad D_{i,i}^c = 0, \ \ (i, j, k = 1, 2, 3), \tag{13}$$

where ρ_1^c is the density of PFRC medium. The density of PFRC medium ρ_1^c, is related to the fibre density (ρ_1^f) and matrix density (ρ_1^m) of the medium through the relation [35]

$$\rho_1^c = \Lambda_f\rho_1^f + (1 - \Lambda_f)\rho_1^m. \tag{14}$$

In the present problem, it is considered that the PFRC medium is acted upon by a horizontal initial stress ℓ_1, parallel to the x_1− axis. Therefore, in light of Eq. (3), Eq. (13) gives

$$\left.\begin{aligned} \sigma_{11,1}^c + \sigma_{13,3}^c + \ell_1(u_{3,13} - u_{1,33}) = \rho_1^c u_{1,tt},\\ \sigma_{13,1}^c + \sigma_{33,3}^c + \ell_1(u_{3,11} - u_{1,13}) = \rho_1^c u_{3,tt},\\ D_{1,1}^c + D_{3,3}^c = 0. \end{aligned}\right\} \tag{15}$$

Substitution of the expressions for the components of stress and electric displacement from Eq. (12) in Eq. (15), yields the non-vanishing mechanical and electrical equations as

$$\begin{aligned} C_{11}^c u_{1,11} + (C_{13}^c + C_{55}^c + \ell_1)u_{3,13} + (C_{55}^c - \ell_1)u_{1,33} + (e_{31}^c + e_{15}^c)\phi_{,13} = \rho_1^c u_{1,tt},\\ (C_{55}^c + \ell_1)u_{3,11} + (C_{55}^c + C_{13}^c - \ell_1)u_{1,13} + C_{33}^c u_{3,33} + e_{15}^c\phi_{,11} + e_{33}^c\phi_{,33} = \rho_1^c u_{3,tt},\\ e_{15}^c u_{3,11} + (e_{15}^c + e_{31}^c)u_{1,13} + e_{33}^c u_{3,33} - \xi_{11}^c\phi_{,11} - \xi_{33}^c\phi_{,33} = 0, \end{aligned} \tag{16}$$

where ϕ is the electrical potential function defined by the expression $E_i^c = -\phi_{,i}$, $(i = 1, 2, 3)$.

According to Snell's law, the apparent wave numbers of the concerned different waves are same, therefore, the solutions of Eq. (16) may be assumed as [36]

$$\{u_1, u_3, \phi\} = \{U_1, U_3, \Phi\}\exp[i\eta(x_1\sin\theta + \alpha x_3 - ct)]. \tag{17}$$

where η is the wavenumber; ω is circular frequency; c is the phase velocity ($=\omega/\eta$); θ is the angle of inclination of wave normal to the axes of symmetry and α is still an unknown. This specific form of the solution (with the convenient inclusion of $\sin\theta$) is general and include results belonging to a variety of layered systems. An important feature of the analysis concerns the manner in which the oblique propagation direction is introduced and the way it modifies the criterion necessary to insure periodicity. If the angle θ is designated (measured from the normal to the interfaces) to define the propagation direction, then this will lead to an explicit dependence of the characteristic equations upon θ.

Now, Eq. (16) when substituted upon by Eq. (17) may be written in the form

Table 1
Symbols and their meaning for the FRC medium.

Symbols	Meaning	Symbols	Meaning
μ_L	longitudinal shear modulus in the preferred direction	$\zeta_{ij} = (v_{j,i} + v_{i,j})/2$	components of infinitesimal strain
μ_T	transverse shear modulus in the preferred direction	γandβ	specific stress components to take into account different layers for concrete part of the composite material
τ_{ij}	components of stress	$a_i (i = 1, 2, 3)$	components of preferred direction of reinforcement$\vec{a}$
δ_{ij}	Kronecker delta	λ	Lame's constant of elasticity

$$\begin{bmatrix} \Psi_{11} & \Psi_{12} & \Psi_{13} \\ \Psi_{21} & \Psi_{22} & \Psi_{23} \\ \Psi_{31} & \Psi_{32} & \Psi_{33} \end{bmatrix} \begin{bmatrix} U_1 \\ U_3 \\ \Phi \end{bmatrix} = \begin{bmatrix} 0 \\ 0 \\ 0 \end{bmatrix}, \tag{18}$$

where $\Psi_{ij}(i, j = 1, 2, 3)$ are provided in Appendix.

The non-trivial solution of Eq. (18) is possible provided

$$|\Psi_{ij}| = 0. \tag{19}$$

Eq. (19) is the secular equation for the PFRC medium. The roots $\alpha_i(i = 1, 2, 3, ...,6)$ and the corresponding values of θ_i, of the hexic Eq. (19) may be obtained by using Cardan's method for fixed values of c.

The roots of the hexic Eq. (19) in α, stands for all possible wave modes for a given magnitude of apparent wave speed c. In particular, out of the six values of α, four stand for the bulk waves (two of which are the wave vector with positive projection and the other two with negative projection along x_3 axis) and two values of αstand for the surface wave. Thus, the four bulk waves may be thought of as the incident and reflected waves respectively. The bulk wave corresponding to the complex value of α, with decreasing or increasing amplitudes accompanied with propagation is physically unacceptable in the elastic solid without dissipation.

Keeping this in mind, it is of significance to assume the first, third and fifth root ofα, say α_1, α_3 and α_5, stand for the reflected QP, the reflected QSV and the reflected EA waves; while the second, fourth and sixth root of α, say α_2, α_4 and α_6, stand for the incident QP, incident QSV and incident EA waves.

In light of Eq. (19), the amplitude ratio of each coupled wave may be defined as

$$G_r^{(1)} = \frac{U_{3r}}{U_{1r}} = \frac{\Psi_{21}(\alpha_r)\Psi_{13}(\alpha_r) - \Psi_{11}(\alpha_r)\Psi_{23}(\alpha_r)}{\Psi_{12}(\alpha_r)\Psi_{23}(\alpha_r) - \Psi_{13}(\alpha_r)\Psi_{22}(\alpha_r)} \tag{20}$$

and

$$H_r^{(1)} = \frac{\Phi_r}{U_{1r}} = \frac{k_{11}(\alpha_r)k_{22}(\alpha_r) - k_{12}(\alpha_r)k_{21}(\alpha_r)}{k_{12}(\alpha_r)k_{23}(\alpha_r) - k_{13}(\alpha_r)k_{22}(\alpha_r)} (r = 1, 2, ...,6). \tag{21}$$

Therefore, the components of displacement, the electric potential, the components of stresses and the electric displacements may be written in terms of $G_r^{(1)}$ and $H_r^{(1)}$ as

$$\begin{aligned} \{u_1, u_3, \phi\} &= \{1, G_\varsigma^{(1)}, H_\varsigma^{(1)}\}U_{1\varsigma}\exp[i\eta(\sin\theta_\varsigma x_1 + \alpha_\varsigma x_3 - ct)] \\ &+ \textstyle\sum_{r=1,3,5}\{1, G_r^{(1)}, H_r^{(1)}\}U_{1r}\exp[i\eta(\sin\theta_r x_1 + \alpha_r x_3 - ct)], \end{aligned} \tag{22}$$

$$\begin{aligned} &\{\sigma_{11}^c, \sigma_{33}^c, \sigma_{31}^c, D_1^c, D_3^c\} \\ &\quad = i\eta\{F_{1\varsigma}^{(1)}, F_{2\varsigma}^{(1)}, F_{3\varsigma}^{(1)}, F_{4\varsigma}^{(1)}, F_{5\varsigma}^{(1)}\}U_{1\varsigma}\exp[i\eta(\sin\theta_\varsigma x_1 + \alpha_\varsigma x_3 - ct)] \\ &+ \textstyle\sum_{r=1,3,5} i\eta\{F_{1r}^{(1)}, F_{2r}^{(1)}, F_{3r}^{(1)}, F_{4r}^{(1)}, F_{5r}^{(1)}\}U_{1r}\exp[i\eta(\sin\theta_r x_1 + \alpha_r x_3 - ct)], \end{aligned} \tag{23}$$

where $F_{jr}^{(1)}(j = 1, 2, ...,5)$ are provided in Appendix. Here, ς can take values 2, 4 and 6 corresponding to incident qP, qSV and EA waves, respectively.

6. Dynamics of the FRC medium under initial stress

The non-vanishing equations of motion, without body force, for the FRC medium may be obtained by using Eqs. (4) and (11) as

$$P_1 v_{1,11} + (Q_1 + \ell_2)v_{3,13} + (R_1 - \ell_2)v_{1,33} = \rho_2 v_{1,tt}, \tag{24}$$

$$(R_1 + \ell_2)v_{3,11} + (Q_1 - \ell_2)v_{1,13} + P_2 v_{3,33} = \rho_2 v_{3,tt}, \tag{25}$$

where

$$P_1 = \lambda + 2\gamma + \beta + 4\mu_L - 2\mu_T,\ Q_1 = \lambda + \gamma + \mu_L,\ P_2 = \lambda + 2\mu_T,\ R_1 = \mu_L. \tag{26}$$

Now, the solution of the Eqs. (24) and (25) may be assumed in the form

$$\{v_1, v_3\} = \{V_1, V_3\}\exp\{i\eta(\sin\theta^* x_1 + \alpha^* x_3 - ct)\}, \tag{27}$$

where α^* and $\theta^*$are quantities analogous to $\alpha$and θ but associated with the medium of refraction (FRC medium).

Substitution of Eq. (27) in Eqs. (24) and (25), and then proceeding as before yields

$$\begin{bmatrix} \psi_{11} & \psi_{12} \\ \psi_{21} & \psi_{22} \end{bmatrix} \begin{bmatrix} V_1 \\ V_3 \end{bmatrix} = \begin{bmatrix} 0 \\ 0 \end{bmatrix}, \tag{28}$$

which for existence of non-trivial solution leads to

$$|\psi_{mn}| = 0, \tag{29}$$

where $\psi_{mn}(m, n = 1, 2)$ are provided in Appendix.

Eq. (29) is a fourth order polynomial equation in α^* for a given magnitude of c. Among the four roots of the equation, two stand for the bulk waves and the other two stand for the surface wave. So, it is assumed that α_2 and α_4 stand for the refracted QP and the refracted QSV waves, respectively.

Again, in light of Eq. (29), the amplitude ratio of each part wave in the FRC medium may be defined as

$$G_p^{(2)} = -\frac{\psi_{11}}{\psi_{12}}(p = 2, 4). \tag{30}$$

Therefore, the components of displacement and stresses may be written as

$$\{v_1, v_3\} = \sum_{p=2,4}\{1, G_p^{(2)}\}V_{1p}\exp\{i\eta(\sin\theta_p^* x_1 + \alpha_p^* x_3 - ct)\}, \tag{31}$$

$$\{\tau_{11}, \tau_{33}, \tau_{31}\} = \sum_{p=2,4} i\eta\{F_{1p}^{(2)}, F_{2p}^{(2)}, F_{3p}^{(2)}\}V_{1p}\exp\{i\eta(\sin\theta_p^* x_1 + \alpha_p^* x_3 - ct)\}, \tag{32}$$

where $F_{jp}^{(2)}(j = 1, 2, 3)$ are provided in Appendix.

7. Boundary conditions and solution of the problem

For the sake of obtaining the suitable boundary conditions at the loosely bonded interface of the considered media, Eq. (2) may be rewritten as

$$\sigma_{13}^c = i\eta C_{55}^c \frac{\Theta}{\sin\theta_\varsigma}\sqrt{\frac{C_{11}^c + 2C_{55}^c}{C_{55}^c}}(u_1 - v_1), (\varsigma = 2, 4, 6), \tag{33}$$

where $\Theta = \frac{\chi\beta_2}{h\mu_T}$.

Now, Θ may be conveniently rewritten as

$$\Theta = \frac{\Omega}{1 - \Omega}, \tag{34}$$

so that the range $0 \leqslant \Theta < \infty$ is now mapped to $0 \leqslant \Omega \leqslant 1$ and Ω may be called as the bonding parameter.

Therefore, the boundary conditions at the loosely bonded common interface (i.e. at $x_3 = 0$) of the two media are as follows:

Electrical boundary conditions at $x_3 = 0$ is:

$$\phi = 0. \tag{35}$$

Mechanical boundary conditions at $x_3 = 0$ are:

$$u_3 = v_3, \tag{36}$$

$$(1 - \Omega)\sigma_{13}^c = i\eta C_{55}^c \frac{\Omega}{\sin\theta_\varsigma}\sqrt{\frac{C_{11}^c + 2C_{55}^c}{C_{55}^c}}(u_1 - v_1), (\varsigma = 2, 4, 6), \tag{37}$$

$$\sigma_{33}^c = \tau_{33}, \tag{38}$$

$$\sigma_{13}^c = \tau_{13}. \tag{39}$$

The following points can be adduced from the meticulous examination of boundary condition (37):

- Ω must attain the numerical value 1 for the case when the PFRC medium is in welded contact to the FRC medium, which modifies the boundary condition (37) to

$$u_1 = v_1. \tag{40}$$

Eq. (40) implies the continuity of displacement at the common interface of the media which is a boundary condition when two medium are in a welded contact.

- Ω must attain the numerical value 0 for the case when the PFRC medium is in smooth contact to the FRC medium, so that the boundary condition (37) reduces to

$$\sigma_{13}^{c} = 0. \tag{41}$$

Eq. (41) is the boundary condition indicating that the shear stress vanishes at the common interface when two medium are in a smooth contact.

- When Ω attains value in between 0 and 1, the two media are said to be loosely bonded to each other i.e. the contact between the medium is not perfect.

Using Eqs. (22), (23), (31) and (32) in the boundary conditions (31)–(32), it may be obtained that

$$\begin{bmatrix} H_1^{(1)} & H_3^{(1)} & H_5^{(1)} & 0 & 0 \\ G_1^{(1)} & G_3^{(1)} & G_5^{(1)} & -G_2^{(2)} & -G_4^{(2)} \\ L_1 & L_3 & L_5 & M & M \\ F_{21}^{(1)} & F_{23}^{(1)} & F_{25}^{(1)} & -F_{22}^{(2)} & -F_{24}^{(2)} \\ F_{31}^{(1)} & F_{33}^{(1)} & F_{35}^{(1)} & -F_{32}^{(2)} & -F_{34}^{(2)} \end{bmatrix} \begin{bmatrix} U_{11} \\ U_{13} \\ U_{15} \\ V_{12} \\ V_{14} \end{bmatrix} = \begin{bmatrix} H_{\varsigma}^{(1)} \\ G_{\varsigma}^{(2)} \\ F_{3\varsigma}^{(1)} - M \\ F_{2\varsigma}^{(1)} \\ F_{3\varsigma}^{(1)} \end{bmatrix} U_{1\varsigma}, \ (\varsigma = 2, 4, 6), \tag{42}$$

where $M = i\eta C_{55}^{c} \frac{\Theta}{\sin\theta_{\varsigma}} \sqrt{\frac{C_{11}^{c} + 2C_{55}^{c}}{C_{55}^{c}}}$, $(\varsigma = 2, 4, 6)$, $L_r = F_{3r}^{(1)} - M$ $(r = 1, 3, 5)$.

The expression for the reflection/refraction coefficients may be obtained with the aid of Eq. (42) which exhibits the dependency of the coefficients on the various affecting parameters viz. anisotropy, initial stresses and bonding parameter.

8. Computational results and discussion

The reflection and refraction coefficients for different values of incident angle (θ or θ_0), made by the incident plane wave at the interface of the two media, is computed numerically with an aim to study the effect of anisotropy, initial stresses and bonding parameter on these coefficients. The material constants of PZT-5H composite is taken for the PFRC medium (M_1) and that of carbon fibre-epoxy resin composite for the FRC medium (M_2). Moreover, for the purpose of comparative study, three different cases of the upper half-space and two cases of the lower half-space is taken into consideration. The data taken for the purpose of numerical computation are provided in Tables 2 and 3.

8.1. Effect of angle of incidence on the reflection and refraction coefficients

Figs. 2–6 are plotted to study the effect of initial stresses acting in both the media and bonding parameter associated with the loosely bonded interface, on the coefficients of reflected and refracted waves. Particularly, Figs. 2-6 depict the variation of reflection coefficient of qP wave(U_{11}/U_{12}), reflection coefficient of qSV wave (U_{13}/U_{12}), reflection coefficient of EA wave (U_{15}/U_{12}), refraction coefficient of qP wave (V_{12}/U_{12}), refraction coefficient of qSV wave (V_{14}/U_{12}), respectively, against the incident angle, θ_0(in radian). The incident angle ranges from 0° to 90° i.e. $0 < \theta_0 < 1.57$ (in radians). Meticulous examination of all the figures conclude that the reflection and refraction coefficients respond differently to the varying magnitude of incident angle.

Fig. 2 suggests that the reflection coefficient U_{11}/U_{12} firstly increase, attains a maximum value and then decreases with increase in the magnitude of incident angle. Fig. 3 manifests that the reflection coefficient U_{13}/U_{12} evidently decreases with increase in the magnitude of the incident angle whereas Fig. 4 reveals that the reflection coefficient U_{15}/U_{12}increases continuously with the increase in incident angle throughout the range $0° < \theta_0 < 90°$. It is reported through Figs. 5 and 6 that refraction coefficients V_{12}/U_{12} and V_{14}/U_{12}, respectively, are affected significantly for small variation in the magnitude of incident angle whereas for higher range, it approaches to settle down to a fixed value.

8.2. Effect of initial stress (l_1) on the reflection and refraction coefficients

In Fig. 2(i), Fig. 3(i), Fig. 4(i), Fig. 5(i) and Fig. 6(i), reflection and refraction coefficients are plotted against the incident angle for different values of horizontal initial stress(l_1) acting in the PFRC medium. In these figures, the negative values of initial stress i.e. $l_1 = -0.4,\ -0.2$ (curves 1 and 2), correspond to tensile initial stress; the positive values of initial stress i.e. $l_1 = 0.4,\ 0.2$ (curves 4 and 5), correspond to compressive initial stress; and $l_1 = 0$(curve 3) represents the case of no initial stress acting in the PFRC medium. All the figures elucidate that the reflection coefficients U_{11}/U_{12} and U_{15}/U_{12} evidently increase; but the reflection coefficient U_{13}/U_{12} and refraction coefficients V_{12}/U_{12} and V_{14}/U_{12} decrease, with increase in initial stress associated with the PFRC medium. The impact of initial stress l_1, on the reflection coefficientU_{11}/U_{12} is found negligible for extreme low and high values of the incident angle; whereas it is significant in the region $17° < \theta_0 < 74°$. On the other hand, the effect of initial stress l_1, on other coefficients i.e. U_{13}/U_{12}, U_{15}/U_{12}, V_{12}/U_{12} and V_{14}/U_{12}, is nearly unnoticed for extreme low value of the incident angle but considerable toward the higher values.

The cases of presence of horizontal tensile initial stress as well as horizontal compressive initial stress may be numerically compared to the case when there is no initial stress acting in the upper semi-infinite medium. Subtle examination of the Fig. 2(i), Fig. 3(i), Fig. 4(i), Fig. 5(i) and Fig. 6(i) establishes that for a fixed value of $\theta_0 = 29°$ (say) or 0.5 rad, there is 0.7% and 1.5% decrease in reflection coefficient of qP wave; 0.88% and 1.79% increase in reflection coefficient of qSV wave; 0.84% and 1.68% decrease in reflection coefficient of EA wave; 0.92% and 1.79% increase in refraction coefficient of qP wave; 0.87% and 1.74% increase in refraction coefficient of qSV wave, when horizontal tensile initial stress $\ell_1 = -0.2$ and -0.4, respectively, compared with the case when $\ell_1 = 0$. Moreover, again for$\theta_0 = 29°$, there is 0.8% and

Table 2
Material properties for medium M_1 and medium M_2.

Materials	Elastic constants($\times 10^9$ N/m^2)	Piezoelectric constants(C/m^2)	Dielectric constants($\times 10^{-9}$ C^2/Nm^2), Densities(kg/m^3)
PZT-5H composites for the PFRC medium (M_1)[22]	$C_{11}^{c} = 151$, $C_{12}^{c} = 98$, $C_{13}^{c} = 96$, $C_{33}^{c} = 124$, $C_{44}^{c} = C_{55}^{c} = 23$.	$e_{31}^{c} = -5.1$, $e_{33}^{c} = 27$, $e_{15}^{c} = e_{24}^{c} = 17$.	$\xi_{11}^{c} = 15.05$, $\xi_{33}^{c} = 13.27$, $\rho_1^{c} = 5407$.
Carbon fibre-epoxy resin composite for the FRC medium (M_2) [15]	$\mu_L = 5.66$, $\mu_T = 2.46$, $\lambda = 5.65$, $\alpha = -1.28$, $\beta = 220.90$.		$\rho_2 = 3321$.

Table 3
Material constants of medium M_1 and medium M_2 associated with special cases of the problem.

Materials	Elastic constants($\times 10^9$ N/m^2)	Piezoelectric constants(C/m^2)	Dielectric constants ($\times 10^{-9}$ C^2/Nm^2), Densities(kg/m^3)
For medium (M_1) as transversely isotropic piezoelectric medium composed of PZT-5H [37]	$C_{11}^f = 126$, $C_{12}^f = 79.5$, $C_{13}^f = 84.1$, $C_{33}^f = 117$, $C_{44}^f = C_{55}^f = 23.$	$e_{31}^f = -6.5$, $e_{33}^f = 23.3$, $e_{15}^f = e_{24}^f = 17.$	$\xi_{11}^f = 15.05$, $\xi_{33}^f = 13.02$, $\rho_1^f = 7500.$
For medium M_1 as isotropic half-space [38]	$\mu_1 = 32.3$, $\lambda_1 = 42.9$ ($C_{12}^c = C_{13}^c = \lambda_1$, $C_{11}^c = C_{33}^c = \lambda_1 + 2\mu_1$, $C_{44}^c = \mu_1$).		$\rho_1 = 2802.$
For medium M_2 as isotropic half-space [38]	$\mu_2 = 71.0$, $\lambda_2 = 64.2$ ($\mu_L = \mu_T = \mu_2$, $\lambda = \lambda_2$, $\alpha = \beta = 0$).		$\rho_2 = 3321.$

1.7% increase in reflection coefficient of qP wave; 0.88% and 1.77% decrease in reflection coefficient of qSV wave; 0.84% and 1.75% increase in reflection coefficient of EA wave; 0.80% and 1.73% decrease in refraction coefficient of qP wave; 0.87% and 1.74% decrease in refraction coefficient of qSV wave, when horizontal compressive initial stress $\ell_1 = 0.2$ and 0.4, respectively, compared with the case when $\ell_1 = 0$.

8.3. Effect of initial stress (l_2) on the reflection and refraction coefficients

In Fig. 2(ii), Fig. 3(ii), Fig. 4(ii), Fig. 5(ii) and Fig. 6(ii), reflection and refraction coefficients are plotted against the incident angle for different values of horizontal initial stress(l_2) associated with the FRC medium where $l_2 = -0.4$, -0.2 correspond to tensile initial stress; $l_2 = 0.4$, 0.2 correspond to compressive initial stress; and $l_2 = 0$ represents the case of no initial stress. It is established from the figures that the existence of initial stress in the FRC medium increases the magnitude of the coefficients U_{11}/U_{12}, U_{15}/U_{12}, V_{12}/U_{12} and V_{14}/U_{12}; but decreases the reflection coefficient U_{13}/U_{12}. The impact of initial stress l_2, on the coefficients U_{11}/U_{12}, U_{13}/U_{12} and U_{15}/U_{12} is considerable for low values i.e. in the range ($0° < \theta_0 < 29°$) of the incident angle;

whereas its influence on the coefficients V_{12}/U_{12} and V_{14}/U_{12} is found significant throughout the range ($0° < \theta_0 < 90°$) of the incident angle. In fact, among all the coefficients, the effect of initial stress l_2 is most prominently observed on the refraction coefficients V_{12}/U_{12} and V_{14}/U_{12}.

The cases of presence of horizontal tensile initial stress and horizontal compressive initial stress associated with the FRC medium, may be compared the case of absence of initial stress in the medium, in terms of percentage increase/decrease. It may be observed that for $\theta_0 = 29°$, there is 0.9% and 2.0% decrease in reflection coefficient of qP wave; 0.99% and 2.28% increase in reflection coefficient of qSV wave; 0.98% and 2.17% decrease in reflection coefficient of EA wave; 9.84% and 18.65% increase in refraction coefficient of qP wave; 11.86% and 28.81% decrease in refraction coefficient of qSV wave, in Fig. 2(ii), Fig. 3(ii), Fig. 4(ii), Fig. 5(ii) and Fig. 6(ii), when horizontal tensile initial stress $\ell_2 = -0.2$ and -0.4, respectively, compared with the case when no initial stress is acting in the lower semi-infinite medium i.e. $\ell_2 = 0$. Again for $\theta_0 = 29°$, there is 0.7% and 1.3% increase in reflection coefficient of qP wave; 0.88% and 1.62% decrease in reflection coefficient of qSV wave; 0.77% and 1.44% increase in reflection coefficient of EA wave; 11.39% and 24.35% decrease in refraction coefficient of qP wave; and 12.71% and 22.03% increase in refraction coefficient of qSV wave, when horizontal compressive initial stress $\ell_2 = 0.2$ and 0.4, respectively, compared with the case when $\ell_2 = 0$.

8.4. Effect of bonding parameter (Ω) on the reflection and refraction coefficients

The reflection and refraction coefficients are plotted against the incident angle for different values of bonding parameter(Ω) in Fig. 2(iii), Fig. 3(iii), Fig. 4(iii), Fig. 5(iii) and Fig. 6(iii). In these figures, curves 1 (for $\Omega \to 0$) and curve 6 (for $\Omega \to 1$) imply the case of smooth contact and perfect bonding of the media, respectively. Apart from these, curves 2, 3, 4 and 5 correspond to the values of bonding parameter(Ω) lying between 0 and 1 i.e. $\Omega = 0.2$, 0.4, 0.6and 0.8, respectively, which interpret the case when the two media are loosely bonded to each other.

Subtle observation of the figures illuminate that the reflection coefficients U_{11}/U_{12} and U_{15}/U_{12} decrease up to $\Omega = 0.6$ and then suddenly increase for $\Omega = 0.8$. On the other hand, the reflection coefficient U_{13}/U_{12} increase up to $\Omega = 0.6$ and then suddenly decrease for $\Omega = 0.8$. Significant effect of the bonding parameter is observed for lower magnitude of the angle of incidence whereas the effect is found to be negligible towards the higher values of the incident angle.

Fig. 5(iii) and Fig. 6(iii) portray that the increase in the magnitude of bonding parameter from $\Omega = 0.2$ to $\Omega = 0.6$is responsible for a decrease in the refraction coefficients V_{12}/U_{12} and V_{14}/U_{12}, which seems to be unexpectedly increased for $\Omega = 0.8$ and $\Omega \to 1$. It is also observed that the value of refraction coefficients fluctuates abruptly for the smaller range of incident angle 0°–3.5° but settle down asymptotically to a constant value as incident angle increases beyond $\theta_0 = 3.5°$.

The percentage increase/decrease of the curves 1, 3, 4, 5 and 6 with respect to curve 2, may present some interesting result, for a fixed value of the incident angle. An analysis of Fig. 2(iii), Fig. 3(iii), Fig. 4(iii), Fig. 5(iii) and Fig. 6(iii) establishes that for $\theta_0 = 63°$ there is 0.1%, 1.03% and 1.60% increment in reflection coefficient of qP wave; 0.26%, 1.82% and 0.78% decrement in reflection coefficient of qSV wave; 0.13%, 1.34% and 1.01% increment in reflection coefficient of EA wave; 20%, 126.66% and 120% increment in refraction coefficient of qP wave; 15%, 110% and 70% increment in refraction coefficient of qSV wave, when the bonding parameter takes values $\Omega \to 0$, $\Omega = 0.8$ and $\Omega \to 1$, respectively, as compare to the case when $\Omega = 0.2$. Similarly it may be marked that, in comparison to the case when $\Omega = 0.2$, there is 0.65% and 8.19% decrement in reflection coefficient of qP wave; 0.52% and 10.02% increment in reflection coefficient of qSV wave; 0.40% and 8.69% decrement in reflection coefficient of EA wave; 46.66% and 266.66% decrement in refraction coefficient of qP wave; and 20% and 215% decrement in refraction coefficient of qSV wave, when the bonding parameter (Ω) takes the values 0.4 and 0.6, respectively, for $\theta_0 = 63°$.

8.5. Effect of anisotropy on the reflection and refraction coefficients

A comparative study of five different cases is performed through each of the figures in Fig. 7 with a view to study the effect of anisotropy on the reflection and refraction coefficients. In each of the figures i.e. Fig. 7(i)–(v), the cases considered are as follows:

Case I: Composite structure undertaken in the present problem i.e. PFRC semi-infinite medium lying over a FRC semi-infinite medium (curve 1);

Case II: When the upper semi-infinite medium of the composite structure is composed of transversely isotropic piezoelectric material and the lower one is comprised of fibre-reinforced composite (curve 2);

Case III: When the upper semi-infinite medium of the composite structure is comprised of piezoelectric fibre-reinforced composite but the lower medium is of isotropic elastic material (curve 3);

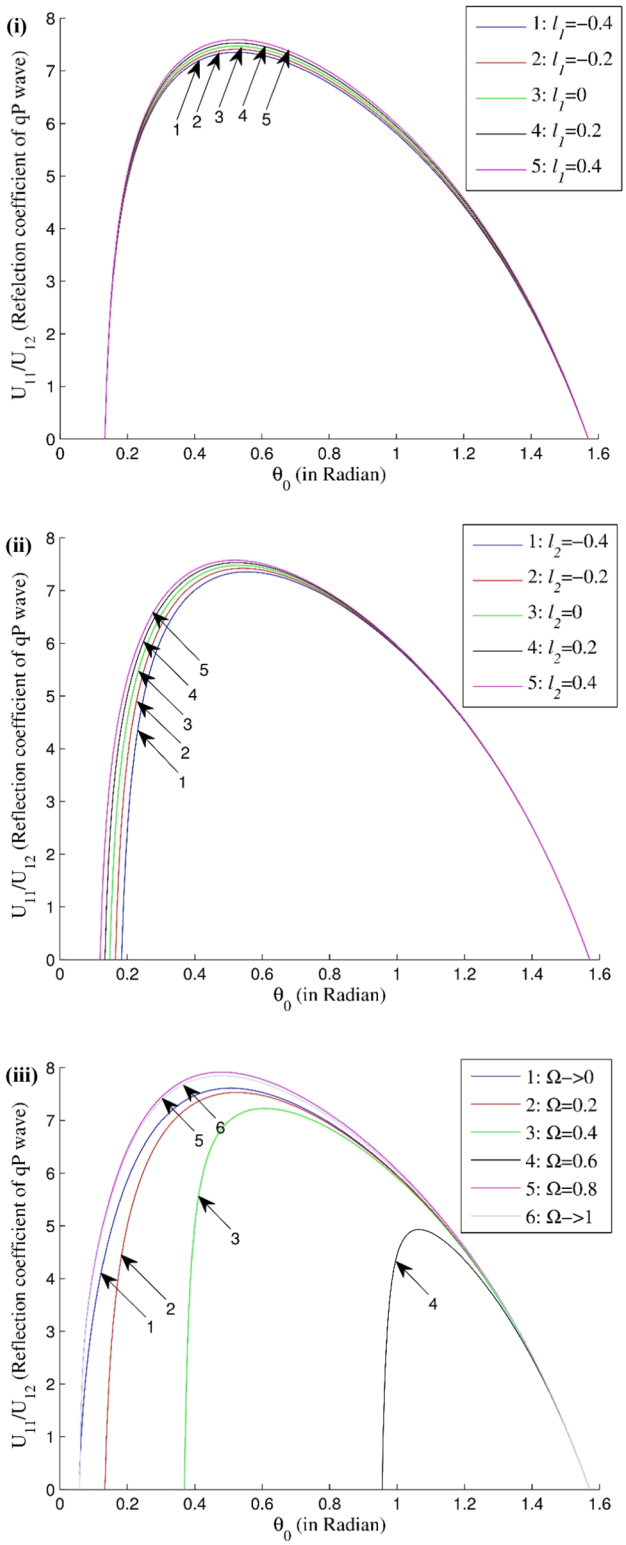

Fig. 2. (i). Scaled reflection coefficient (U_{11}/U_{12}) of reflected qP wave against incident angle for different values of initial stress associated with PFRC medium. 2(ii). Scaled reflection coefficient (U_{11}/U_{12}) of reflected qP wave against incident angle for different values of initial stress associated with FRC medium. 2(iii). Scaled reflection coefficient (U_{11}/U_{12}) of reflected qP wave against incident angle for different values of bonding parameter.

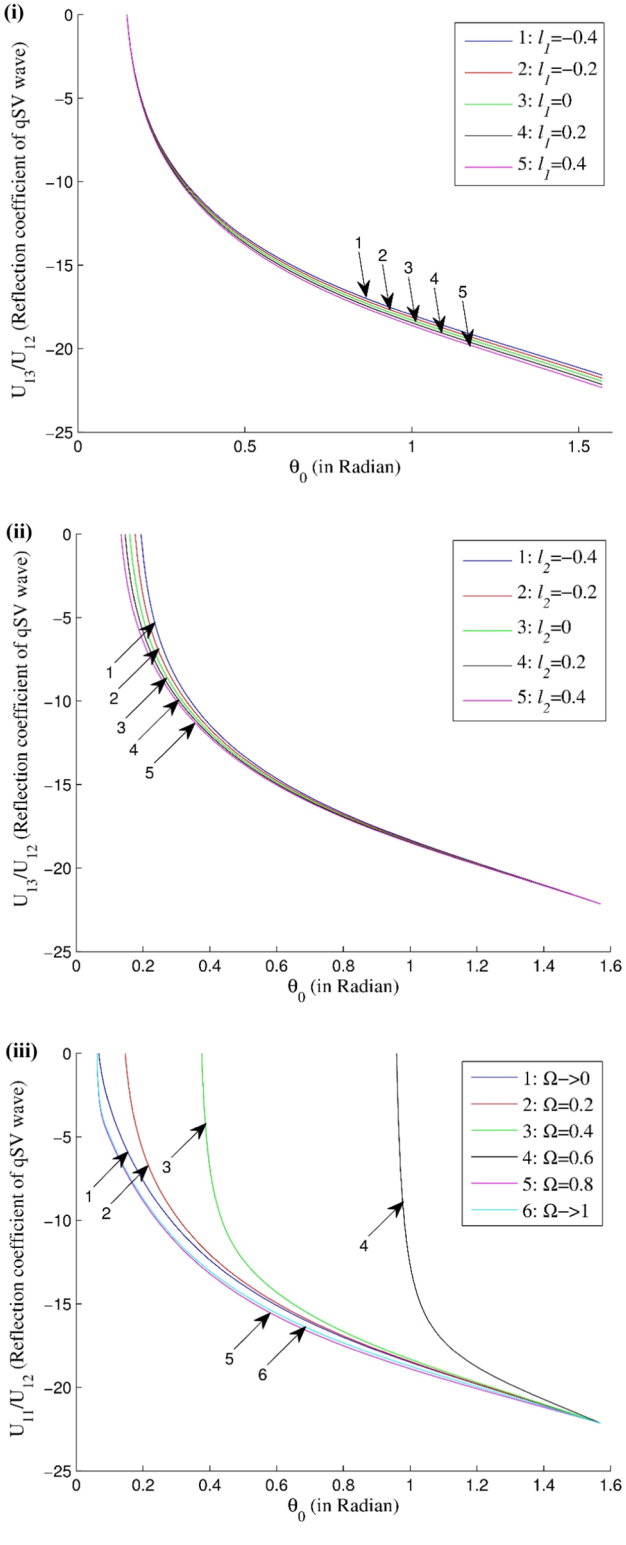

Fig. 3. (i). Scaled reflection coefficient (U_{13}/U_{12}) of reflected qSV wave against incident angle for different values of initial stress associated with PFRC medium. 3(ii). Scaled reflection coefficient (U_{13}/U_{12}) of reflected qSV wave against incident angle for different values of initial stress associated with FRC medium. 3(iii). Scaled reflection coefficient (U_{13}/U_{12}) of reflected qSV wave against incident angle for different values of bonding parameter.

Case IV: When the upper semi-infinite medium of the composite structure is comprised of transversely isotropic piezoelectric material and the lower one is of isotropic elastic material (curve 4);

Case V: When both upper and lower semi-infinite medium of the composite structure is comprised of isotropic elastic material (curve 5).

In particular, Fig. 7(i) shows the variation of reflection coefficient of reflected qP wave (U_{11}/U_{12}) whereas Fig. 7(ii) exhibits the variation of

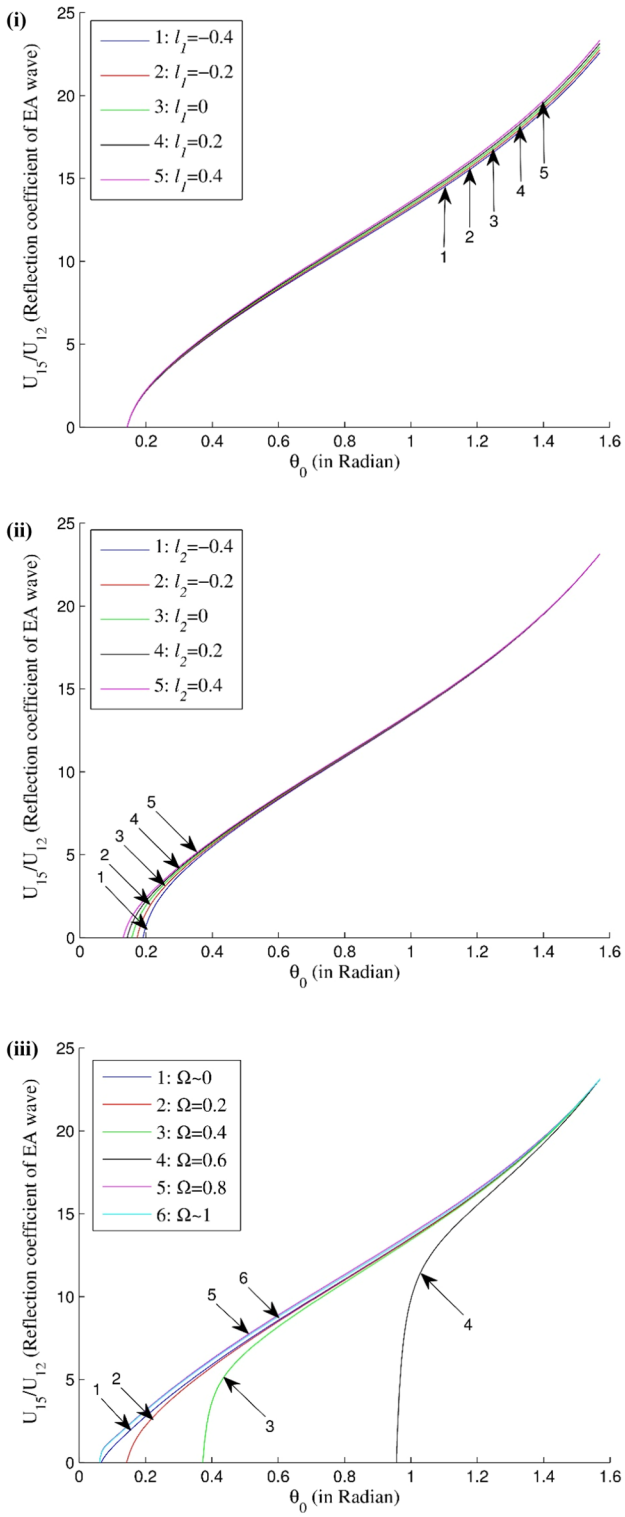

Fig. 4. (i). Scaled reflection coefficient (U_{15}/U_{12}) of reflected EA wave against incident angle for different values of initial stress associated with PFRC medium. 4(ii). Scaled reflection coefficient (U_{15}/U_{12}) of reflected EA wave against incident angle for different values of initial stress associated with FRC medium. 4(iii). Scaled reflection coefficient (U_{15}/U_{12}) of reflected EA wave against incident angle for different values of bonding parameter.

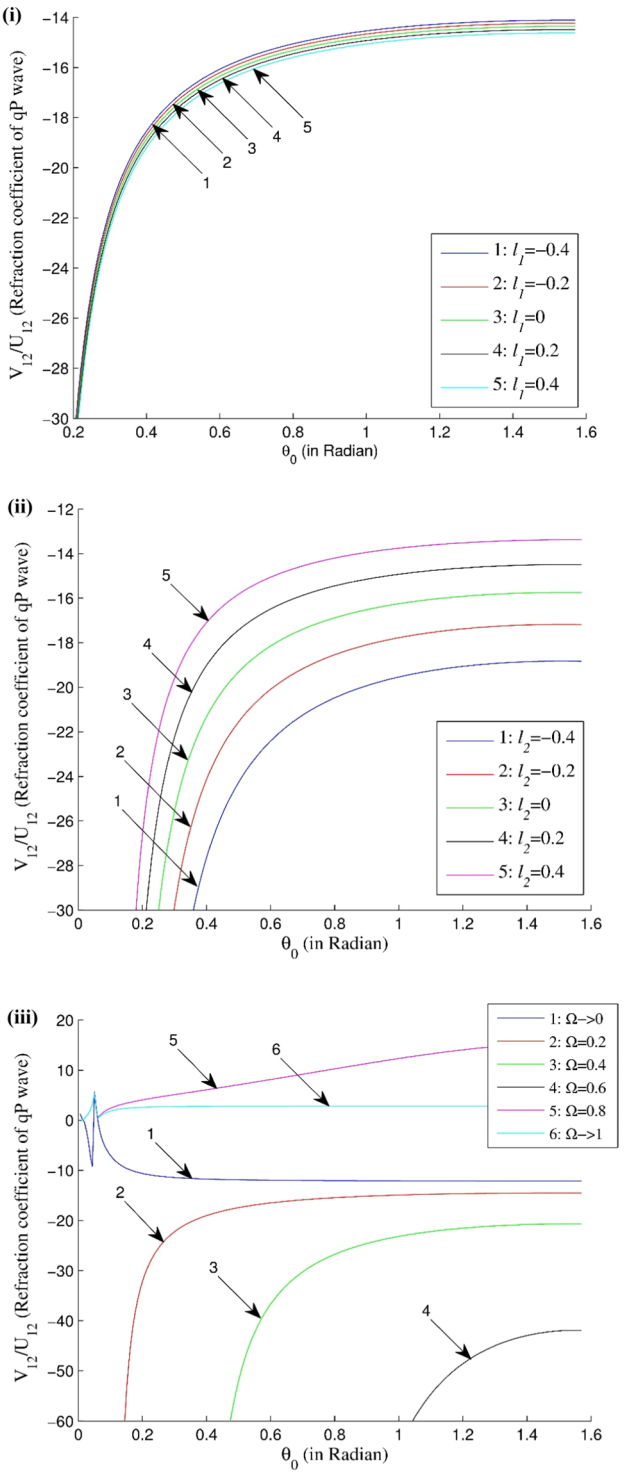

Fig. 5. . (i). Scaled refraction coefficient (V_{12}/U_{12}) of refracted qP wave against incident angle for different values of initial stress associated with PFRC medium. 5(ii). Scaled refraction coefficient (V_{12}/U_{12}) of refracted qP wave against incident angle for different values of initial stress associated with FRC medium. 5(iii). Scaled refraction coefficient (V_{12}/U_{12}) of refracted qP wave against incident angle for different values of bonding parameter.

reflection coefficient of reflected qSV wave (U_{13}/U_{12}), against the angle of incidence for the aforementioned cases. For all the cases, the reflection coefficient (U_{11}/U_{12}) firstly increase for the range $0° < \theta_0 < 29°$ and then decrease; while the reflection coefficient (U_{13}/U_{12}) decreases throughout $0° < \theta_0 < 90°$, with increase in the angle of incidence. The figures set forth that for a fixed value of incident angle (say at $\theta_0 = 29°$), the reflection coefficient (U_{11}/U_{12}) is maximum while the reflection coefficient (U_{13}/U_{12}) is minimum, for the case when composite structure is comprised of isotropic elastic material only (Case V). Fig. 7(iii) expounds the variation of reflection coefficient of EA wave(U_{15}/U_{12})

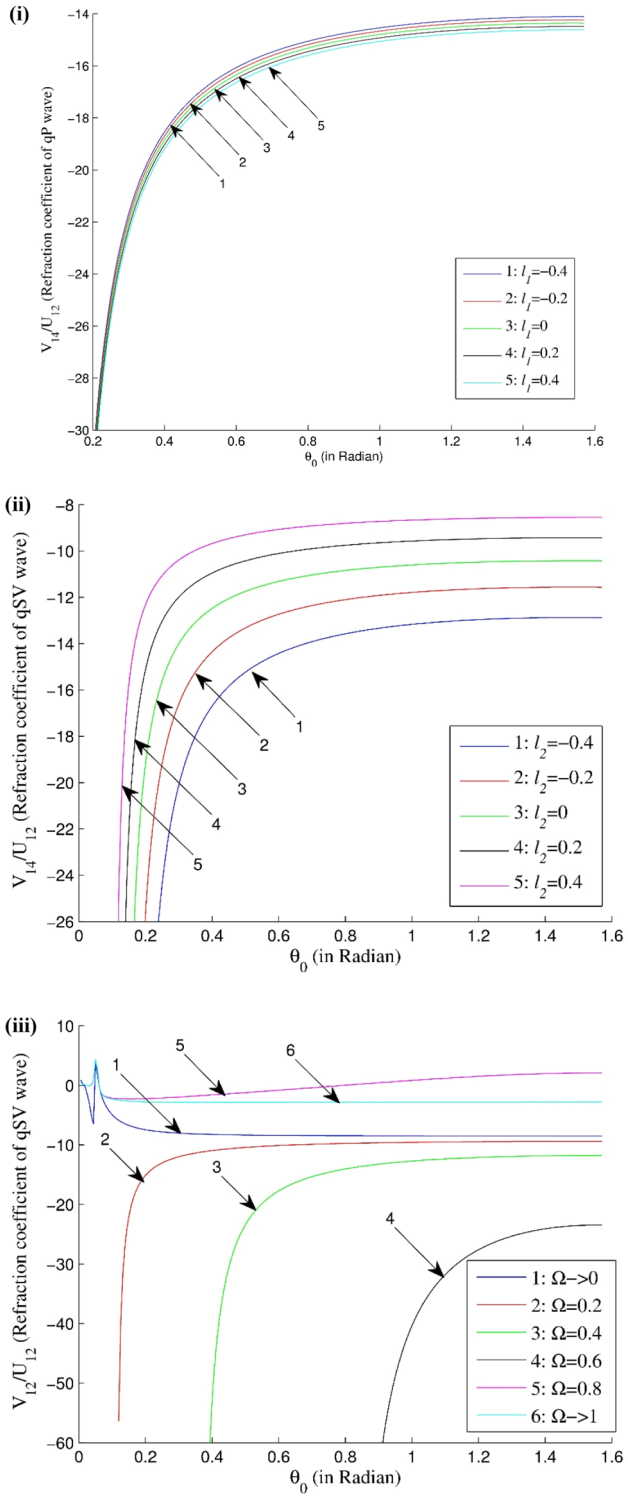

Fig. 6. (i). Scaled refraction coefficient (V_{14}/U_{12}) of reflected qSV wave against incident angle for different values of initial stress associated with PFRC medium. 6(ii). Scaled refraction coefficient (V_{14}/U_{12}) of reflected qSV wave against incident angle for different values of initial stress associated with FRC medium. 6(iii). Scaled refraction coefficient (V_{14}/U_{12}) of reflected qSV wave against incident angle for different values of bonding parameter.

against the incident angle. It may be observed from the figure that the curve corresponding to Case V behave differently in the beginning but finally, as like other curves of other cases (Case I, II, III and IV), which embark on a continuous increasing trend, the reflection coefficient (U_{15}/U_{12})also increases with the increase in incident angle.

Comparative study of curves 1, 2, 3 and 4 in Fig. 7(i) and (iii) manifests that the presence of reinforcement in the lower semi-infinite medium discourages the reflection coefficients of qP wave (U_{11}/U_{12}) and EA wave (U_{15}/U_{12}) in the lower range of incident angle, but this effect remain unnoticed for higher range of incident angle. As long as reinforcement prevail in the upper semi-infinite medium of the composite structure along with piezoelectricity, the coefficients (U_{11}/U_{12}) and (U_{15}/U_{12}) retain higher magnitude in the range $23° < \theta_0 < 90°$ as compare to the case when the piezoelectric medium is reinforced free, irrespective of the fact the lower semi-infinite medium is reinforced or reinforced free. It is remarkably traced out that discouraging effect of presence reinforcement in lower semi-infinite medium dominates over the discouraging effect of presence of reinforcement in the upper semi-infinite medium on the said reflection coefficients of reflected waves. Fig. 7(ii) suggest that the aforementioned trends seem to be antagonistic for the reflection coefficient (U_{13}/U_{12}).

Fig. 7(iv) and (v) render the variation of refraction coefficient of qP wave (V_{12}/U_{12}) and refraction coefficient of qSV wave (V_{14}/U_{12}), respectively, against the incident angle for the aforementioned cases. Both the figures reveal the distinct characteristic of the coefficients for different cases. Minute observation of the curves 1, 2, 3 and 4 in Fig. 7(iv) and (v) enlightens that the presence of reinforcement in either of the semi-infinite media discourages the refraction coefficients V_{12}/U_{12} and V_{14}/U_{12}. It is worthy to mention here that the discouraging effect of prevalence of reinforcement in the upper piezoelectric semi-infinite medium is more as compare to the presence of reinforcement in the lower semi-infinite medium. Apart from this, curve 5 in both the figures, associated with Case V, shows a totally different behaviour at lower magnitude of incident angle but decreases with increase in incident angle for the range $29° < \theta_0 < 90°$. Particularly, the refraction coefficient of both qP and qSV waves for case V, attain peak value at $\theta_0 = 25°$ and then decreases with increase in incident angle.

Therefore, an overview of all the figures conclude that all the coefficients are considerably affected by the presence/absence of reinforcement in either of the medium, but the effect of reinforcement prevailing in the upper medium on the reflection and refraction coefficients is indispensable.

9. Slowness section

In order to study the effect of anisotropy on the slowness curves of the upper PFRC medium in x_1x_3-plane (as shown in Fig. 8) the solutions in Eq. (17) are re-written in the form

$$\{u_1, u_3, \phi\} = \{U_1, U_3, \Phi\} \exp[i\omega(S_1x_1 + S_3x_3 - t)], \tag{43}$$

where $\omega(=\eta c)$ is the angular frequency and

$$S_1 = \sin\theta c^{-1}, \quad S_3 = \alpha c^{-1}. \tag{44}$$

Substitution of Eq. (43) into Eq. (16), with the condition that the procured homogeneous system admits a non-trivial solution, yields the equation of the associated slowness section.

In Fig. 8, curve 1 corresponds to the case when the upper medium is PFRC medium; curve 2 is associated to the case when the upper medium become transversely isotropic piezoelectric; and curve 3 interpret the case when the upper medium is isotropic. It is observed that none of the curves are coinciding to each other which concludes that anisotropy present in the medium have significant effect on the slowness curves.

10. Energy partition

Consider a thin layer at the interface of the two media, with length $l_{x_1} \times l_{x_3}$ and infinitesimal thickness δ such that $\delta \to 0$. The normal energy flux balance within this thin layer requires that the sum of the energy reflection and refraction coefficients is unity. Therefore, the energy carried by the incident wave and the energy dividing between the reflected and the refracted waves are estimated as follows:

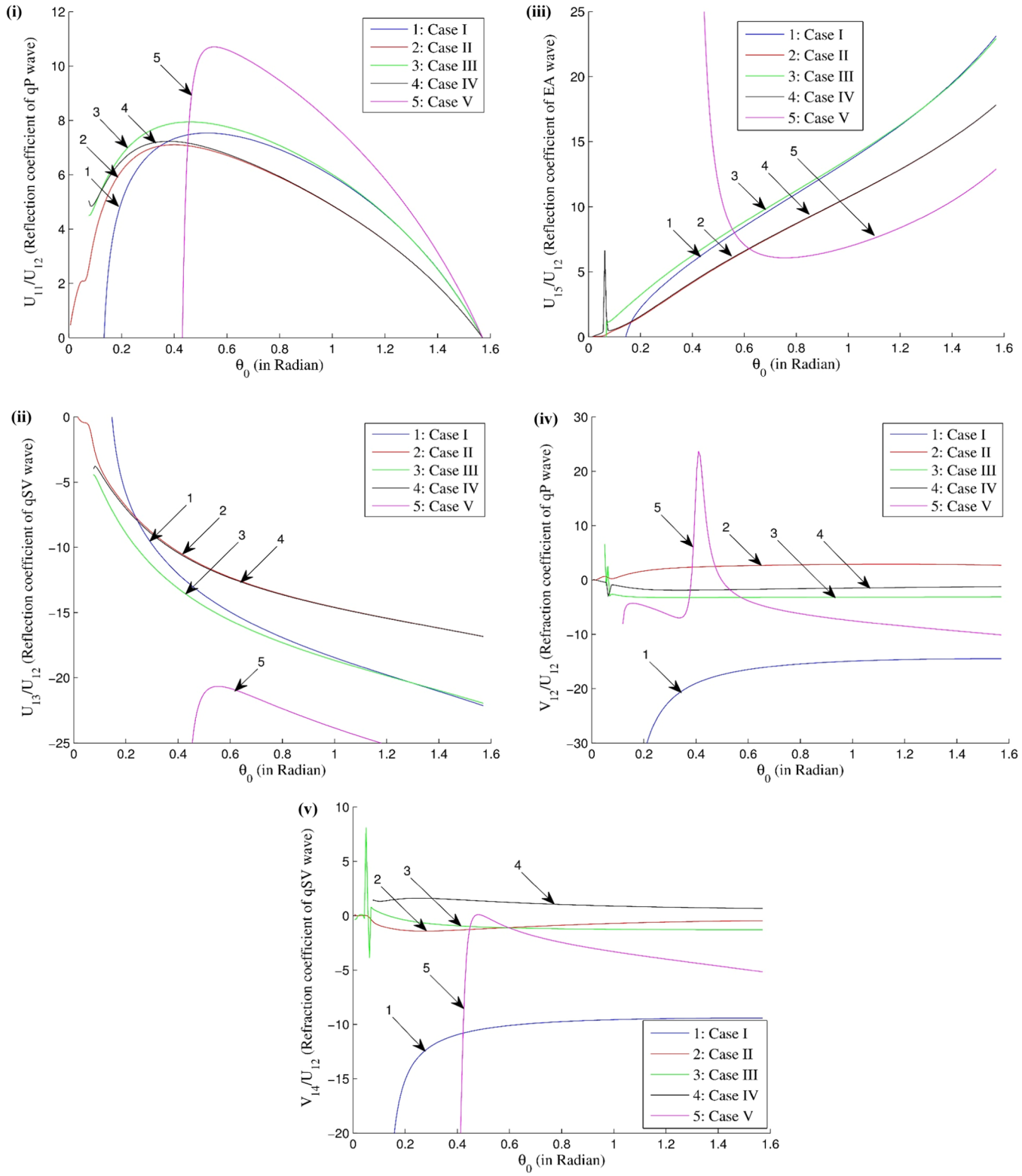

Fig. 7. (i). Incident angle against scaled reflection coefficient (U_{11}/U_{12}) of reflected qP wave for distinct special cases. 7(ii). Incident angle against scaled reflection coefficient (U_{13}/U_{12}) of reflected qSV wave for distinct special cases. 7(iii). Incident angle against scaled reflection coefficient (U_{15}/U_{12}) of reflected EA wave for distinct special cases. 7(iv). Incident angle against scaled refraction coefficient (V_{12}/U_{12}) of refracted qP wave for distinct special cases. 7(v). Incident angle against scaled refraction coefficient (V_{14}/U_{12}) of refracted qSV wave for distinct special cases.

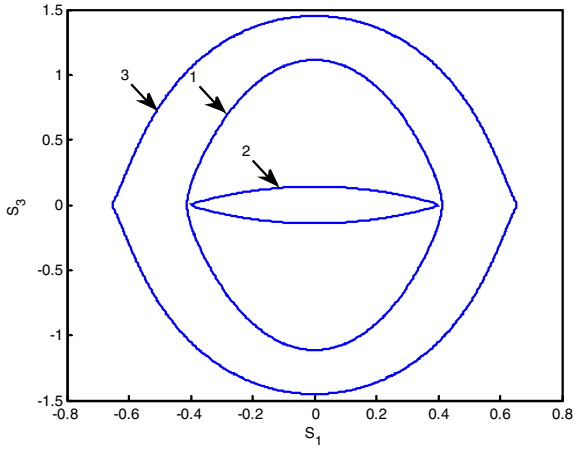

Fig. 8. Slowness surface.

For all real values of the physical quantities, the energy flux density carried by a coupled wave may be given as

$$\mathrm{X}_i(t) = -\dot{u}_j\sigma_{ji}^{c} - \ell_{ik}u_{j,k}\dot{u}_j + \phi\dot{D}_i^{c}, \tag{45}$$

which implies that the averaged energy flux in one period is

$$\bar{\mathrm{X}}_i = \frac{\omega}{2\pi}\int_{-\pi/\omega}^{\pi/\omega}\mathrm{X}_i(t)dt. \tag{46}$$

In light of Eq. (46), it may be written that

$$\bar{\mathrm{X}}_i = \frac{1}{2}\mathrm{Re}(-\dot{u}_j^{*}\sigma_{ji}^{c} - \ell_{ik}u_{j,k}\dot{u}_j^{*} + \phi\dot{D}_i^{c*}). \tag{47}$$

The superscript "$*$" in $\dot{u}_j^{*}$ and $\dot{D}_i^{c*}$ alludes the conjugated complex of the physical quantities $\dot{u}_j$ and $\dot{D}_i^{c}$ respectively. Substitution of Eqs. (22), (23), (31) and (32) into Eq. (47), the averaged energy flux through unit area vertical to the propagation direction for the incident wave and the reflection wave may be obtained as

$$\bar{\mathrm{X}}_{x_1r} = \frac{1}{2}\eta^2 c[F_{1r}^{(1)} + G_r^{(1)*}F_{3r}^{(1)} + \ell_1(1 + G_r^{(1)}G_r^{(1)*}) + H_r^{(1)}F_{4r}^{(1)*}](U_{1r}\cdot U_{1r}^{*}), \tag{48}$$

$$\bar{\mathrm{X}}_{x_3r} = \frac{1}{2}\eta^2 c[F_{3r}^{(1)} + G_r^{(1)*}F_{2r}^{(1)} + H_r^{(1)}F_{5r}^{(1)*}](U_{1r}\cdot U_{1r}^{*}), \tag{49}$$

and for the refraction wave may be procured as

$$\bar{\mathrm{X}}_{x_1p} = \frac{1}{2}\eta^2 c[F_{1p}^{(2)} + G_p^{(2)*}F_{3p}^{(2)} + \ell_2(1 + G_p^{(2)}G_p^{(2)*})](V_{1p}\cdot V_{1p}^{*}), \tag{50}$$

$$\bar{\mathrm{X}}_{x_3p} = \frac{1}{2}\eta^2 c[F_{3p}^{(2)} + G_p^{(2)*}F_{2p}^{(2)}](V_{1p}\cdot V_{1p}^{*}), \tag{51}$$

where $r = 1(\text{or } 2 \text{ or } 3)$, 4, 5, 6 and $p = 2$, 4.

Further, the energy flux along the propagation direction $\boldsymbol{n}_d$ is

$$\bar{\mathrm{X}}_d = \bar{\mathrm{X}}_{nd} = \bar{\mathrm{X}}_{x_1d}\cos(\boldsymbol{n}_d, x_1) + \bar{\mathrm{X}}_{x_3d}\cos(\boldsymbol{n}_d, x_3),\ (d = p, r). \tag{52}$$

Now, define the energy reflection and refraction coefficients as the ratio of energy flux of the reflection and refraction waves to the incident wave, i.e.

$$\mathrm{E}_{qP}^{RE} = \frac{\bar{\mathrm{X}}_{qP}^{RE}}{\bar{\mathrm{X}}_{qP(qSV)}^{I}},\ \mathrm{E}_{qSV}^{RE} = \frac{\bar{\mathrm{X}}_{qSV}^{RE}}{\bar{\mathrm{X}}_{qP(qSV)}^{I}},\ \mathrm{E}_{EA}^{RE} = \frac{\bar{\mathrm{X}}_{EA}^{RE}}{\bar{\mathrm{X}}_{qP(qSV)}^{I}},\ \mathrm{E}_{qP}^{RF} = \frac{\bar{\mathrm{X}}_{qP}^{RF}}{\bar{\mathrm{X}}_{qP(qSV)}^{I}},\ \mathrm{E}_{qSV}^{RF} = \frac{\bar{\mathrm{X}}_{qSV}^{RF}}{\bar{\mathrm{X}}_{qP(qSV)}^{I}}, \tag{53}$$

it may be established that

$$\mathrm{E} = (\bar{X}_{x_3qP}^{RE} + \bar{X}_{x_3qSV}^{RE} + \bar{X}_{x_3EA}^{RE} + \bar{X}_{x_3qP}^{RF} + \bar{X}_{x_3qSV}^{RF})/\bar{X}_{x_3qP(qSV)}^{I} = 1, \tag{54}$$

where the superscripts I, RE and RF stands for the incident, reflected and refracted waves, respectively.

The condition in Eq. (54) validates the obtained results of the current study.

11. Concluding remarks

The present paper formulated the problem of reflection and refraction due to the incidence of plane waves at the loosely bonded common interface of an initially stressed PFRC medium and an initially stressed FRC medium. The expression for the amplitude ratios are obtained, which established their dependency on various affecting parameters. Hence, the effect of anisotropy, initial stresses, loose bonding and reinforcement on the amplitude ratios are studied numerically and demonstrated by means of graphs. The prime outcomes of the study are encapsulated as follows:

- The reflection and refraction coefficients are greatly affected by the change in angle of incidence. In particular, the lower magnitudes of incident angle favor, but the higher magnitudes disfavor the reflection coefficient of qP wave. The reflection coefficient of EA wave and the refraction coefficients of qP and qSV waves are highly encouraged with the incident angle, while the reflection coefficient of qSV wave is discouraged.
- The reflection coefficients of qP and EA waves are favored by the presence of initial stresses in either of the media; but the reflection coefficient of qSV wave and the refraction coefficient of qP wave are disfavored. Besides this, the refraction coefficient of qSV wave is disfavored by the initial stress prevailing in the PFRC medium, and favored by the initial stress existing in the FRC medium.
- All the reflection and refraction coefficients, except the reflection coefficient of qSV wave, attain higher magnitude for the extreme cases, i.e. when the media are either in welded contact or in smooth contact with each other. On the other hand, the said coefficients evidently decreases for the case when the two media are loosely bonded to each other.
- The reinforcement prevailing in the PFRC medium encourages the reflection coefficient of qP and EA waves, while the reflection coefficient of qSV wave is discouraged. Contrariwise, the presence of reinforcement in the FRC medium discourages the reflection coefficient of qP and EA waves, while the reflection coefficient of qSV wave is encouraged. The reinforcement present in the upper semi-infinite medium (PFRC medium) significantly affects the reflection and refraction coefficients as compare to presence of reinforcement in the lower medium (FRC medium).
- All the reflection and refraction coefficients are most affected for the case when both the semi-infinite medium are without reinforcement. In particular, the reflection coefficient of qP wave attains the highest values and the reflection coefficients of qSV and EA waves attain the lowest values in the range $28° < \theta° < 90°$,for the said case.
- The anisotropy present in both the medium significantly affects the slowness curves. It is also established that the sum of the energy reflection and refraction coefficients is unity. This validates the numerical results of the current study.

The problems of reflection and refraction of plane waves at the common interface of two dissimilar media may find its possible applications in many fields including geophysics, acoustics, non-destructive evaluation, mining in oil industries, earthquake engineering, etc. Such phenomenon may be of great importance to geophysicists for exploration of various materials buried beneath the earth's surface and in determining the gross earth structures, especially, the crustal (including the oceanic crust) and upper mantle structures. The study of reflection and refraction in piezoelectric composites are helpful in medical imaging applications, sensor technology and in designing memory devices, smart structures, underwater transducers, etc. Particularly, the present study may prove its worthiness in modeling the propagation characteristics of plane wave generated through artificial explosion of the

layered piezoelectric reinforced structures to study the energy transmission in the model with a view to attain best performance out of it.

Acknowledgements

Authors convey their sincere thanks to Department of Science and Technology, Science & Engineering Research Board (DST-SERB) for their financial support to carry out this research work through Project no. EMR/2016/003985/MS entitled “Mathematical Study on Wave Propagation Aspects in Piezoelectric Composite Structures with Complexities”.

Appendix

$\boldsymbol{\sigma}^{\Gamma} = \left[\begin{array}{cccccc}\sigma_{11}^{\Gamma} & \sigma_{22}^{\Gamma} & \sigma_{33}^{\Gamma} & \sigma_{23}^{\Gamma} & \sigma_{13}^{\Gamma} & \sigma_{12}^{\Gamma}\end{array}\right]^{\mathrm{T}}$, $\boldsymbol{\varepsilon}^{\Gamma} = \left[\begin{array}{cccccc}\varepsilon_{11}^{\Gamma} & \varepsilon_{22}^{\Gamma} & \varepsilon_{33}^{\Gamma} & 2\varepsilon_{23}^{\Gamma} & 2\varepsilon_{13}^{\Gamma} & 2\varepsilon_{12}^{\Gamma}\end{array}\right]^{\mathrm{T}}$,

with $\varepsilon_{ij}^{c} = \frac{1}{2}(u_{i,j} + u_{i,j})$, $(i, j = 1, 2, 3)$.

$\boldsymbol{D}^{\Gamma} = [D_1^{\Gamma} \;\; D_2^{\Gamma} \;\; D_3^{\Gamma}]$, $\boldsymbol{E}^{\Gamma} = [E_1^{\Gamma} \;\; E_2^{\Gamma} \;\; E_3^{\Gamma}]$,

$$\boldsymbol{C}^{\Gamma} = \begin{bmatrix} C_{11}^{\Gamma} & C_{12}^{\Gamma} & C_{13}^{\Gamma} & 0 & 0 & 0 \\ C_{12}^{\Gamma} & C_{22}^{\Gamma} & C_{23}^{\Gamma} & 0 & 0 & 0 \\ C_{13}^{\Gamma} & C_{23}^{\Gamma} & C_{33}^{\Gamma} & 0 & 0 & 0 \\ 0 & 0 & 0 & C_{44}^{\Gamma} & 0 & 0 \\ 0 & 0 & 0 & 0 & C_{55}^{\Gamma} & 0 \\ 0 & 0 & 0 & 0 & 0 & C_{66}^{\Gamma} \end{bmatrix}, \quad \boldsymbol{e}^{\gamma} = \begin{bmatrix} 0 & 0 & e_{31}^{\gamma} \\ 0 & 0 & e_{32}^{\gamma} \\ 0 & 0 & e_{33}^{\gamma} \\ 0 & e_{24}^{\gamma} & 0 \\ e_{15}^{\gamma} & 0 & 0 \\ 0 & 0 & 0 \end{bmatrix}, \quad \boldsymbol{\xi}^{\Gamma} = \begin{bmatrix} \zeta_{11}^{\Gamma} & 0 & 0 \\ 0 & \xi_{22}^{\Gamma} & 0 \\ 0 & 0 & \xi_{33}^{\Gamma} \end{bmatrix},$$

where $\Gamma = f,\ m,\ c$ and $\gamma = f,\ c$. $C_{11}^{c} = \left(\Lambda_f C_{11}^{f} + \Lambda_m C_{11}^{m} + \frac{q_1 a_1 + q_5 a_2}{D}\right)$, $C_{12}^{c} = \left(C_{12}^{m} + \frac{q_2 a_1 + q_6 a_2}{D}\right)$, $C_{13}^{c} = \left(C_{13}^{f} + \frac{q_1 c_{23}^{f} + q_5 c_{33}^{f}}{D}\right)$, $C_{22}^{c} = \left(\frac{q_2 C_{22}^{f} + q_6 C_{23}^{f}}{D}\right)$, $C_{23}^{c} = \left(\frac{q_3 c_{22}^{f} + q_7 c_{23}^{f}}{D}\right)$, $c_{33}^{c} = \left(\frac{q_3 c_{23}^{f} + q_7 c_{33}^{f}}{D}\right)$, $\frac{1}{c_{ii}^{c}} = \frac{\Lambda_f}{c_{ii}^{f}} + \frac{\Lambda_m}{c_{ii}^{m}} (i = 4, 5, 6)$, $e_{31}^{c} = \Lambda_f e_{31}^{f} - \left(\frac{q_4 a_1 + q_8 a_2}{D}\right)$, $e_{32}^{c} = e_{32}^{f} - \left(\frac{q_4 C_{23}^{f} + q_8 C_{33}^{f}}{D}\right)$, $e_{33}^{c} = e_{33}^{f} - \left(\frac{q_4 C_{23}^{f} + q_8 C_{33}^{f}}{D}\right)$, $e_{15}^{c} = e_{15}^{f}\left(1 - \frac{\Lambda_m c_{55}^{f}}{\Lambda_f c_{55}^{m} + \Lambda_m c_{55}^{f}}\right)$, $e_{24}^{c} = e_{24}^{f}\left(1 - \frac{\Lambda_m C_{44}^{f}}{\Lambda_f C_{44}^{m} + \Lambda_m C_{44}^{f}}\right)$, $\xi_{33} = \Lambda_f \xi_{33}^{p} + \Lambda_m \xi_{33}^{m} + \Lambda_f\left(\frac{q_4 e_{32}^{f} + q_8 e_{33}^{f}}{D}\right)$, $D = (\Lambda_m C_{22}^{f} + \Lambda_f C_{22}^{m})(\Lambda_m C_{33}^{f} + \Lambda_f C_{33}^{m}) - (\Lambda_m C_{23}^{f} + \Lambda_f C_{23}^{m})^2$, $a_1 = \Lambda_f (C_{12}^{f} - C_{12}^{m})$, $a_2 = \Lambda_f (C_{13}^{f} - C_{13}^{m})$, $q_1 = \Lambda_m (C_{13}^{f} - C_{13}^{m})(\Lambda_m C_{23}^{f} + \Lambda_f C_{23}^{m}) - \Lambda_m (C_{12}^{f} - C_{12}^{m})(\Lambda_m C_{33}^{f} + \Lambda_f C_{33}^{m})$, $q_2 = C_{22}^{m}(\Lambda_m C_{33}^{f} + \Lambda_f C_{33}^{m}) - c_{33}^{m}(\Lambda_m C_{23}^{f} + \Lambda_f C_{23}^{m})$, $q_3 = C_{23}^{m}(\Lambda_m C_{33}^{f} + \Lambda_f c_{33}^{m}) - c_{33}^{m}(\Lambda_m C_{23}^{f} + \Lambda_f V_{23}^{m})$, $q_4 = \Lambda_m e_{32}^{f}(\Lambda_m C_{33}^{f} + \Lambda_f C_{33}^{m}) - \Lambda_m e_{33}^{f}(\Lambda_m C_{23}^{f} + \Lambda_f C_{23}^{m})$, $q_5 = -\Lambda_m (C_{13}^{f} - C_{13}^{m})(\Lambda_m C_{22}^{f} + \Lambda_f C_{22}^{m}) + \Lambda_m (C_{12}^{f} - C_{12}^{m})(\Lambda_m C_{23}^{f} + \Lambda_f C_{23}^{m})$, $q_6 = -C_{22}^{m}(\Lambda_m C_{23}^{f} + \Lambda_f C_{23}^{m}) + C_{23}^{m}(\Lambda_m C_{22}^{f} + \Lambda_f C_{22}^{m})$, $q_7 = -C_{23}^{m}(\Lambda_m C_{23}^{f} + \Lambda_f C_{23}^{m}) + C_{33}^{m}(\Lambda_m C_{22}^{f} + \Lambda_f C_{22}^{m})$, $q_8 = -\Lambda_m e_{31}^{f}(\Lambda_m C_{23}^{f} + \Lambda_f C_{23}^{m}) + \Lambda_m e_{33}^{f}(\Lambda_m C_{22}^{f} + \Lambda_f C_{22}^{m})$, $\Psi_{11} = C_{11}^{c} + \alpha^2 C_{55}^{c} - \alpha^2 \ell_1 - \rho_1^{c} c^2$, $\Psi_{12} = \alpha C_{13}^{c} + \alpha C_{55}^{c} + \alpha \ell_1$, $\Psi_{13} = \alpha e_{31}^{c} + \alpha e_{15}^{c}$, $\Psi_{21} = \alpha (C_{55}^{c} + C_{13}^{c} - \ell_1)$, $\Psi_{22} = C_{55}^{c} + \ell_1 + \alpha^2 C_{33}^{c} - \rho_1 c^2$, $\Psi_{23} = e_{15}^{c} + \alpha^2 e_{33}^{c}$, $\Psi_{31} = e_{15}^{c}(\alpha + 1) + \alpha e_{31}^{c}$, $\Psi_{32} = \alpha^2 e_{33}^{c}$, $\Psi_{33} = -\xi_{11}^{c} - \alpha \xi_{33}^{c}$, $F_{1r}^{(1)} = C_{11}^{c} + \alpha_r^{(1)} G_r^{(1)} C_{13}^{c} - c e_{31}^{c} H_r^{(1)} \alpha_r^{(1)}$, $F_{2r}^{(1)} = C_{13}^{c} + C_{33}^{c} G_r^{(1)} \alpha_r^{(1)} - c e_{33}^{c} H_r^{(1)} \alpha_r^{(1)}$, $F_{3r}^{(1)} = C_{55}^{c}(G_r^{(1)} + \alpha_r^{(1)}) + e_{15}^{c} H_r^{(1)}$, $F_{4r}^{(1)} = e_{15}^{c}(G_r^{(1)} + \alpha_r^{(1)}) - \xi_{11}^{c} H_r^{(1)}$, $F_{5r}^{(1)} = e_{31}^{c} + e_{33}^{c} H_r^{(1)} \alpha_r^{(1)} - \xi_{33}^{c} H_r^{(1)} \alpha_r^{(1)}$, $\psi_{11} = P_1 + \alpha^{*2}(R_1 - \ell_2) - \rho_2 c^2$, $\psi_{12} = \alpha^{*}(Q_1 - \ell_2)$, $\psi_{21} = \alpha^{*}(Q_1 + \ell_2)$, $\psi_{22} = R_1 + \ell_2 + \alpha^{*2} P_2 + \rho_2 c^2$, $F_{1p}^{(2)} = P_1 + (Q_1 - \mu_L)\alpha_p^{*} G_p^{(2)}$, $F_{2p}^{(2)} = Q_1 - \mu_L + P_2 \alpha_p^{*} G_p^{(2)}$, $F_{3p}^{(2)} = R_1 \alpha_p^{*} + R_1$.

References

[1] C.M. Keith, S. Crampin, Seismic body waves in anisotropic media: reflection and refraction at a plane interface, Geophys. J. Int. 49 (1) (1977) 181–208.
[2] M. Chatterjee, S. Dhua, S.A. Sahu, A. Chattopadhyay, Reflection in a highly anisotropic medium for three-dimensional plane waves under initial stresses, Int. J. Eng. Sci. 85 (2014) 136–149.
[3] A. Chattopadhyay, P. Kumari, V.K. Sharma, Reflection and transmission of a three-dimensional plane qP wave through a layered fluid medium between two distinct triclinic half-spaces, Int. J. Geomech. 14 (2) (2013) 182–190.
[4] C. Modi, P. Kumari, V.K. Sharma, Reflection/refraction of qP/qSV wave in layered self-reinforced media, App. Math. Mod. 40 (19) (2016) 8737–8749.
[5] S.J. Singh, S. Khurana, Reflection and transmission of P and SV waves at the interface between two monoclinic elastic half-spaces, Proc. National Acad. Sci.- India 71 (2001) 305–319.
[6] V. Thapliyal, Reflection of SH-waves from anisotropic transition layer, Bull Seismol. Soc. Am. 64 (1974) 1979–1991.
[7] G.S. Murty, Theoretical model for the attenuation and dispersion of Stoneley waves at the loosely-bonded interface of elastic half-spaces, Phys. Earth Planet Inter. 11 (1975) 65–79.
[8] G.S. Murty, Reflection, transmission and attenuation of elastic waves at a loosely bonded interface of two half-spaces, Geophys. J. Roy Astron. Soc. 44 (1976) 389–404.
[9] B. Singh, S. Singh, Reflection and transmission of elastic waves at a loosely bonded interface between an elastic solid and a viscoelastic porous solid saturated by viscous liquid, Global J. Res. Eng. (2014) 14(3).
[10] B. Singh, R. Kumar, Reflection and refraction of micropolar elastic waves at a loosely bonded interface between viscoelastic solid and micropolar elastic solid, Int. J. Eng. Sci. 36 (2) (1998) 101–117.
[11] J.S. Nandal, T.N. Saini, Reflection and refraction at an imperfectly bonded interface between poroelastic solid and cracked elastic solid, J. Seismol. 17 (2) (2013) 239–253.
[12] P.C. Vinh, P.T.H. Giang, On formulas for the velocity of Stoneley waves propagating along the loosely bonded interface of two elastic half-spaces, Wave Motion 48 (7) (2011) 647–657.
[13] A.K. Singh, Z. Parween, A. Das, A. Chattopadhyay, Influence of loosely-bonded sandwiched initially stressed visco-elastic layer on torsional wave propagation, J. Mech. 33 (3) (2016) 351–368.
[14] B. Singh, Wave propagation in thermally conducting linear fibre-reinforced composite materials, Arch. App. Mech. 75 (2006) 513–520.
[15] A. Chattopadhyay, A.K. Singh, Propagation of magnetoelastic shear waves in an irregular self-reinforced layer, J. Eng. Math. 75 (2012) 139–155.
[16] S.K. Samal, R. Chattaraj, Surface wave propagation in fiber-reinforced anisotropic elastic layer between liquid saturated porous half space and uniform liquid layer, Acta Geophys. 59 (3) (2011) 470–482.
[17] A.K. Singh, K.C. Mistri, A. Das, Propagation of love-type wave in a corrugated fibre-reinforced layer, J. Mech. 32 (6) (2016) 693–708.
[18] Y. Pang, Y.S. Wang, J.X. Li, D.N. Fang, Reflection and refraction of plane waves at the interface between piezoelectric and piezomagnetic media, Int. J. Eng. Sci. 46 (11) (2008) 1098–1110.
[19] Y. Pang, J.X. Liu, Reflection and transmission of plane waves at an imperfectly bonded interface between piezoelectric and piezomagnetic media, Eur. J. Mech. A-Solid 30 (5) (2011) 731–740.
[20] A.K. Singh, A. Das, K.C. Mistri, A. Chattopadhyay, Green's function approach to study the propagation of SH-wave in piezoelectric layer influenced by a point source, Math. Method Appl. Sci. 40 (13) (2017) 4771–4784.
[21] M.C. Ray, Micromechanics of piezoelectric composites with improved effective piezoelectric constants, Int. J. Mech. Mat. Des. 3 (2006) 361–371.
[22] N. Mallik, M.C. Ray, Effective Coefficients of Piezoelectric Fiber-Reinforced Composites, AIAA J. 41 (4) (2003) 704–710.
[23] A. Kumar, D. Chakraborty, Effective properties of thermo-electro-mechanically coupled piezoelectric fiber reinforced composites, Mat. Des. 30 (2009) 1216–1222.
[24] V. Kumar, R. Jiwari, Gupta R. Kumar, Numerical simulation of two dimensional quasilinear hyperbolic equations by polynomial differential quadrature method, Eng. Comput. 30 (7) (2013) 892–909.
[25] V. Kumar, R.K. Gupta, R. Jiwari, Comparative study of travelling-wave and numerical solutions for the coupled short pulse (CSP) equation, Chinese Phys. B. 22 (5)

(2013).
[26] R. Jiwari, S. Pandit, R.C. Mittal, Numerical simulation of two-dimensional sine-Gordon solitons by differential quadrature method, Computer Phys. Commun. 183 (3) (2012) 600–616.
[27] A. Verma, R. Jiwari, Cosine expansion based differential quadrature algorithm for numerical simulation of two dimensional hyperbolic equations with variable coefficients, Int. J. Numerical Meth. Heat Fluid Flow 25 (7) (2015) 1574–1589.
[28] A.K. Singh, K.C. Mistri, A. Chattopadhyay, Love-type wave propagation in an irregular prestressed composite sandwiched layer, Int. J. Geomech. 16 (2) (2015).
[29] B. Singh, A.K. Yadav, Reflection of plane waves in an initially stressed perfectly conducting transversely isotropic solid half-space, J. Earth Sys. Sci. 122 (4) (2013) 1045–1053.
[30] A.N. Guz, Elastic waves in bodies with initial (residual) stresses, Int. App. Mech. 38 (1) (2002) 23–59.
[31] P. Khurana, A.K. Vashisth, Love wave propagation in a pre-stressed medium, Indian J. Pure App. Math. 32 (8) (2001) 1201–1208.
[32] R.M. Jones, Mechanics of Composite Materials, 2nd ed., Taylor and Francis, 1999.
[33] Y. Benveniste, G.J. Dvorak, Uniform fields and universal relations in piezoelectric composites, J. Mech. Phy. Solids 40 (6) (1992) 1295–1312.
[34] A.J. Belfield, T.G. Rogers, A.J.M. Spencer, Stress in elastic plates reinforced by fibres lying in concentric circles, J. Mech. Phy. Solids 31 (1) (1983) 25–54.
[35] A. Seema, K.R. Dayas, J.M. Varghese, PVDF-PZT-5H composites prepared by hot press and tape casting techniques, J. App. Polym. Sci. 106 (1) (2007) 146–151.
[36] A.H. Nayfeh, Wave propagation in layered anisotropic media: With application to composites, Elsevier, North-Holland, 1995.
[37] X. Guo, P. Wei, Effects of initial stress on the reflection and transmission waves at the interface between two piezoelectric half spaces, Int. J. Solid Struct. 51 (21) (2014) 3735–3751.
[38] D. Gubbins, Seismology and plate tectonics, Cambridge University Press, Cambridge, U.K., 1990.